

T 14
114

**Attenuation measurement of the backscattered ultrasonic
A-mode signal for beef grading**

ISU
1991
W633
C. 3

by

Lanny B. Widyaatmadja

A Thesis submitted to the
Graduate Faculty in Partial Fulfillment of the
Requirements for the Degree of
MASTER OF SCIENCE
Major: Biomedical Engineering

Signatures have been redacted for privacy

Signatures have been redacted for privacy

Iowa State University
Ames, Iowa
1991

TABLE OF CONTENTS

CHAPTER 1 INTRODUCTION.....	1
Objectives of Study.....	5
CHAPTER 2 LITERATURE REVIEW.....	7
Background in A-Mode Ultrasound.....	7
Background of the Attenuation in Muscle Tissue...	11
Relationship between Attenuation and Frequency...	15
The Least Squares Estimate of Attenuation Slope..	17
CHAPTER 3 EXPERIMENTAL PROCEDURE.....	19
Data Acquisition system.....	19
Pulser/Receiver.....	21
Transducer.....	21
Preparation of Beef Samples.....	25
Precautions Taken During Measurements.....	26
Sampling the A-Mode Signals.....	27
Windowing the A-Mode Signal.....	28
Frequency Domain Processing.....	29
Mean Square Linear Regression Method.....	31
Summary of Experimental Steps.....	32

CHAPTER 4 RESULTS AND DISCUSSION.....	34
Signal Processing in 9.18% Fat Sample.....	34
Ether Extraction Analysis (Chemical Test).....	45
Slope of the Attenuation Coefficient of Each Sample.....	46
Attenuation Slope of the Longissimus Dorsi Muscle Sample.....	51
The Observation of the A-Mode Signal.....	52
The Observation in the Power Spectra.....	55
Recommendation.....	61
 BIBLIOGRAPHY.....	 63
 ACKNOWLEDGEMENTS.....	 66
 APPENDIX A. RESULTS OF EXPERIMENTS.....	 67
APPENDIX B. MOISTURE/FAT DETERMINATION (CHANG, 1991)..	77
APPENDIX C. SIGNAL PROCESSING PROGRAM.....	79
APPENDIX D. STATISTICAL ANALYSIS.....	85

LIST OF TABLES

Table 1.1	Mean ether extractable fat content of the longissimus dorsi between the 12th-13th ribs classified according to their marbling level.	5
Table 3.1	Parametric Pulser/Receiver Settings.....	22
Table 4.1	The location of the samples in the longissimus muscle, the percentage fat and the slope of the attenuation coefficient.....	35
Table 4.2	The spectral magnitude from 11 windows at a frequency 1.52 MHz. These data were recorded at 0° angle line of sight from a sample with 9.18% fat.....	42
Table 4.3	The slope of the attenuation coefficient measured from 9 different angles and the percentage of fat of 10 samples.....	48
Table 4.4	The p-values of samples Hypothesis: $\mu_A = \mu_B$ where μ_i = mean value of slope of the attenuation coefficient of sample i.....	49

Table 4.5	Grouping of samples with no significant difference in the mean slopes of the attenuation coefficients.....	51
Table 4.6	The p-values for comparing the slopes of the attenuation coefficient of samples from the longissimus dorsi.....	53

LIST OF FIGURES

Figure 1.1	Illustrates the lower limit of the degree of marbling level in the longissimus muscle between the 12th-13th ribs used as the USDA Standard for beef grading.....	4
Figure 2.1	The incident planar waveform is reflected and transmitted at the boundary of the changing media from medium 1 with acoustic impedance $Z_1 = \rho_1 c_1$ to medium 2 with acoustic impedance $Z_2 = \rho_2 c_2$ where ρ_1 = density of medium 1 and ρ_2 = density of medium 2.....	9
Figure 2.2	Ultrasound echo analysis from different interface boundaries	12
Figure 2.3	Analog A-mode signal from steak of different grades.....	13
Figure 3.1	Functional block diagram of the PC-based data acquisition system.....	20
Figure 3.2	Ultrasound water tank.....	20
Figure 3.3	Characteristic of the transducer (a) Impulse response (b) Frequency response.....	24

Figure 3.4	The sample cut from the longissimus dorsi positioned with the rectangular-shaped broadband transducer for data sampling.....	26
Figure 3.5	Anatomical references of the 12th-13th ribeye steaks. (1) Acorn fat depot, (2) spine, (3) medial end, (4) lateral end, (5) longissimus costarum, (6) proximal border, (7) distal border, and (8) intercostal muscle. Dotted line marks how the samples were cut	27
Figure 3.6	Block diagram of the method used to process the raw backscattered signal.....	33
Figure 4.1	Backscattered signal sampled at 20 MHz from one line of sight (0° angle).....	36
Figure 4.2	Backscattered signal divided into 256-point data segments.....	37
Figure 4.3	Result of zero-padding the first 256-point window segment.....	38
Figure 4.4	The result of FFT without smoothing process (a) power spectrum of a 512-point data segment (b) log power spectrum	38

Figure 4.5	Smoothing process (a) autocorrelation of a backscattered signal from a 512-point window segment (b) 256-point Hamming window (c) the autocorrelation signal filtered by 256-point Hamming window.....	39
Figure 4.6	The result of FFT after smoothing process (a) power spectrum of a 512-point data segment (b) log power spectrum.....	41
Figure 4.7	The linear regression of the data from Table 4.2.....	44
Figure 4.8	The slope of the attenuation coefficient of a 9.18% fat sample at 0° line of sight within the bandwidth 1.52 - 5.00 MHz.....	45
Figure 4.9	The linear fitting of the slope of the attenuation coefficient as a function of % fat.....	47
Figure 4.10	Backscattered signal from one line of sight of sample with fat percentage (a) 9.18 (b) 7.19 (c) 1.52.....	54
Figure 4.11	The 1st segmentation data signal from a sample with percentage fat (a) 9.18 (b) 7.19 (c) 5.12.....	56

Figure 4.12 Frequency response of the 1st window from the sample with percentage fat (a) 9.18 (b) 7.19 (c) 5.12..... 57

Figure 4.13 The correlation between the center frequency and the depth of the sample for a sample with percentage fat (a) 9.18 (b) 7.19 (c) 5.12..... 60

CHAPTER 1. INTRODUCTION

Ultrasound is defined as acoustic waves with frequencies above those that can be detected by the human ear, from about 20 KHz to several hundred MHz. As the frequency is increased, the wavelength of the ultrasound wave becomes progressively smaller. This small wavelength gives the ultrasound wave unique resolution capabilities compared to ordinary sound waves. In addition, ultrasound is considered safe at low power.

Ultrasound imaging has been a fast growing technique for tissue characterization in medicine and in some areas of agriculture. In the medical field, ultrasound provides an image determined by the acoustic properties of the tissue. This complements the information provided by X-Rays and CAT-scanners in which images are based on the atomic number density of the tissue. Also, due to its ability to demonstrate motion and flow, ultrasound is used as a unique tool by cardiologists and obstetricians.

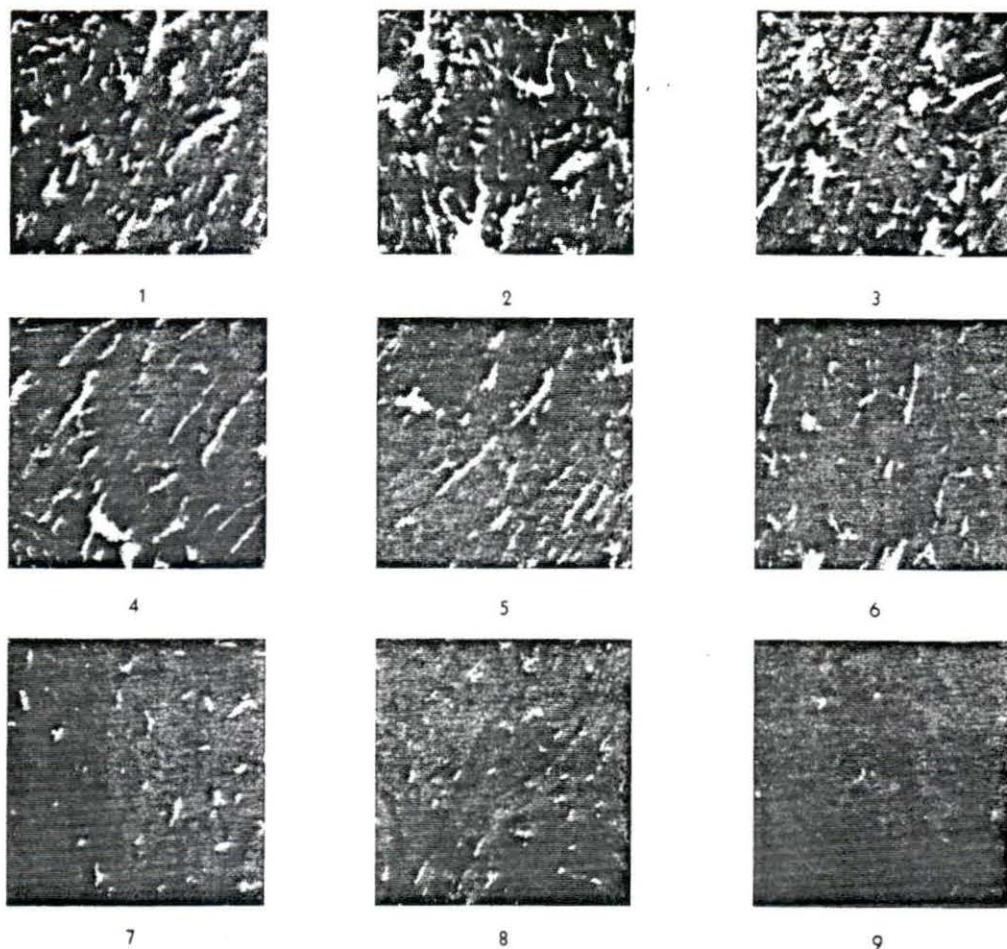
In agriculture, ultrasound has become an important objective measurement device to evaluate many aspects of foods. The technique of measuring the velocity of an ultrasonic wave by timing its passage through a sample of known thickness is used to determine the concentration of a particular food component. This method has been used to determine the quality of food - e.g., the age of an egg, the thickness of an egg's shell, the percentage of solid fat in oil, and the ripeness of fruit. In addition, the attenuation measurement has been used to find the quantities of egg white and egg yolk (Javanaud, 1988).

In the meat industry, ultrasound reflectance techniques have been used to determine fat thickness in beef cattle and swine. Recently, there has been growing interest in using ultrasound to objectively grade beef in the carcass as well as in live cattle. For many years, beef grading has been a subjective process. It has been done by United States Department of Agriculture (USDA) graders who evaluate the intramuscular fat, or marbling, in the longissimus dorsi muscle of the beef carcass which has been split between the 12th and the 13th ribs. Thus, the beef grading depends on the individual judgement of the grader. Although experienced graders are generally consistent in their decisions, there are many marginal cases in which the decisions may not be

consistent. Because this decision is the primary basis for establishing the economic value of the carcass to the rancher, packer and consumer, it is desirable to formulate a methodology to produce an objective, quality grade from the carcass. Recently, it has been suggested that ultrasound can be used to evaluate the marbling fat (Anselmo et al., 1987).

The longissimus dorsi muscle is graded from high to low marbling as US Prime, US Choice, US Good, and US Standard. Figure 1.1 shows the typical visible marbling used as a reference in the official USDA Standard of Grading (Anselmo et al., 1987). Table 1.1 presents means and standard deviations of the fat percentage (based on ether extraction analysis) for the marbling level of the longissimus dorsi muscle between 12th-13th rib.

The most commonly used ultrasound instrument is the B-Mode scanner. B-Mode scan instruments utilize the information of the A-mode scan, together with the position and orientation of the transducer, to construct a two dimensional image. The A-mode is based upon the pulse-echo technique which will be discussed further in Chapter 2. Using a one dimensional imaging A-mode method to determine the tissue characteristics of meat will lower the cost of building an ultrasound instrument to grade meat.



Illustrations adapted from negative furnished by New York State College of Agriculture, Cornell University

- | | |
|------------------------|-----------|
| 1- Very abundant | 6- Modest |
| 2- Abundant | 7- Small |
| 3- Moderately abundant | 8- Slight |
| 4- Slightly abundant | 9- Traces |
| 5- Moderate | |

Figure 1.1 Illustrates the lower limit of the degree of marbling level in the longissimus muscle between the 12th-13th ribs used as the USDA Standard for beef grading

Table 1.1 Mean ether extractable fat content (Savell et al., 1986), of the longissimus dorsi between the 12th-13th ribs classified according to their marbling level (Boggs and Merkel, 1979)

Marbling level	Ether extractable % fat	
	Mean	SD
Prime		
Moderately abundant	10.42	2.16
Slightly abundant	8.56	1.60
Moderate	7.34	1.50
Choice		
Modest	5.97	1.15
Small	4.99	1.10
Good		
slight	3.43	0.89
Standard		
Traces	2.48	0.59
Practically devoid	1.77	1.12

Objectives of Study

The purpose of the work described in this thesis is to determine a method to process the A-mode signal data from the longissimus dorsi muscle between the 12th-13th ribs and to find an appropriate parameter to allow marbling in the samples to be differentiated objectively. The parameter studied in these experiments was the slope of the attenuation coefficient

from the backscattered signal. The slope of the attenuation coefficient is determined by applying the least squares method in the frequency domain. This technique was developed for the quantitative estimation of ultrasound attenuation in the liver (Wilson et al., 1984). Variation of the attenuation with a number of disease states in the liver has been found; e.g., the cirrhotic liver has been reported to show greater attenuation than the normal liver. The objective of this experiment is to apply this method to beef grading and see if a fatty ribeye steak has a greater slope of the attenuation coefficient than a less fatty one. The ultimate goal of this area of research is to build a low-cost and portable real-time system that can electronically determine the carcass grade and possibly predict the grade in live cattle.

CHAPTER 2 LITERATURE REVIEW

Background in A-Mode Ultrasound

The A-mode ultrasound is the amplitude display of the reflected signal as a short pulse of ultrasound is transmitted by the transducer into the tissue regions being investigated. The echo (reflected) signals, due to various boundaries and interfaces within the tissue, are received back at the transducer. Whenever ultrasound waves pass from a region of one impedance value into a neighboring region of different impedance, a certain amount of the incident power is reflected at the boundary, and the remaining part continues as a transmitted wave. In Figure 2.1, i , r , and t refer to incident, reflected and transmitted waves respectively. As in optics, Snell's law applies here:

$$\theta_i = \theta_r \quad \frac{\sin \theta_i}{\sin \theta_r} = \frac{c_1}{c_2}$$

where c_1 = wave velocity in medium 1

and c_2 = wave velocity in medium 2.

The reflection and transmission coefficients can be found by using the boundary condition that the pressure and particle velocity should be continuous across the boundary (Shung, 1987).

$$\frac{P_r}{P_i} = \frac{(Z_2 \cos \theta_i - Z_1 \cos \theta_t)}{(Z_2 \cos \theta_i + Z_1 \cos \theta_t)}$$

and

$$\frac{P_t}{P_i} = \frac{(2 Z_2 \cos \theta_i)}{(Z_2 \cos \theta_i + Z_1 \cos \theta_t)}$$

where P_r/P_i = pressure reflectivity of the interface
 P_t/P_i = pressure transmittivity of the interface
 Z_1 = acoustic impedance of the medium 1
and Z_2 = acoustic impedance of the medium 2.

The characteristics mentioned above make the A-mode pulse echo ultrasound a good one-dimensional mapping display of the tissue interfaces along the line of propagation of the beam. It gives spatial information of the characteristic of the medium investigated. The total transit time from initial pulse to reception of the echo is proportional to the depth of the boundary. This total time needed by the pulse to travel from the transducer and be reflected from a boundary back to the

same transducer is twice the depth of the boundary divided by the average phase velocity of the pulse in the tissue. This total transit time can be calculated as:

$$t = \frac{2 \text{ (depth)}}{c}$$

where $c = 1540 \text{ m/sec.}$

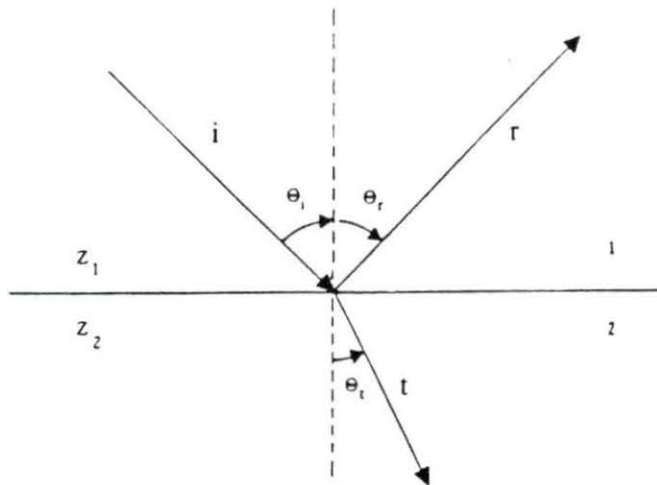


Figure 2.1 The incident planar waveform is reflected and transmitted at the boundary of the changing media from medium 1 with acoustic impedance $Z_1 = \rho_1 c_1$ to medium 2 with acoustic impedance $Z_2 = \rho_2 c_2$ where $\rho_1 =$ density of medium 1 and $\rho_2 =$ density of medium 2.

The ultrasound wave travels at a different velocity everytime it is reflected from a tissue boundary. Thus, it is usually difficult to ascertain the exact tissue velocity. It is assumed that the average tissue phase velocity of the wave has a value between the phase velocity of the wave in water and in muscle. The average phase velocity in soft tissues is 1540 m/sec.

The utility, or use, of the A-mode ultrasound in the agricultural field has been studied by Anselmo et al. (1987). In this study, the A-mode ultrasound was used as a tool to analyze subjectively the relationship between the qualitative appearance of marbling in the 12th and the 13th steak and the "richness" of the ultrasound signature. The data is interpreted with the aid of Figure 2.2. A typical target is assumed to be comprised of two homogeneous substances of different densities which are muscle (shaded) and fat (unshaded). If there are no fat structures within the muscle, one would expect an echo pattern as indicated in the "low fat signature" echo, the only echoes are those resulting from the muscle-external fat interfaces. If the muscle is filled with islands of fat, the resulting echo pattern would be as indicated in the "high fat signature" echo. This assumption (the relative comparison of the "richness" of the echo) is used as a qualitative indicator of marbling within the muscle. The results of using the A-mode to study several meat samples

is shown in Figure 2.3 (Anselmo et al., 1987). A greater ultrasound echo signature is found in higher marbling grades of the beef.

Background of the Attenuation in Muscle Tissue

The attenuation coefficient is described as the loss of energy that occurs when an ultrasonic wave passes through a length of tissue. The dimension of the acoustic attenuation coefficient at a certain frequency is dB/cm. When a wave propagates through an attenuating medium, its energy is reduced as an exponential function of distance traveled by the wave. This is described by the equation:

$$P_z = P_{z0} e^{-A(f)z}$$

where P_{z0} = power at $z=0$

P_z = power at distance z

$A(f)$ = power attenuation coefficient in dB/cm

and z = acoustic path distance wave propagates in tissue.

The attenuation coefficient in biological tissue depends on the elastic properties of the tissue. The attenuation coefficient of an ultrasonic wave in striated muscle tissue is higher than in other soft tissue. The muscle is tightly packed

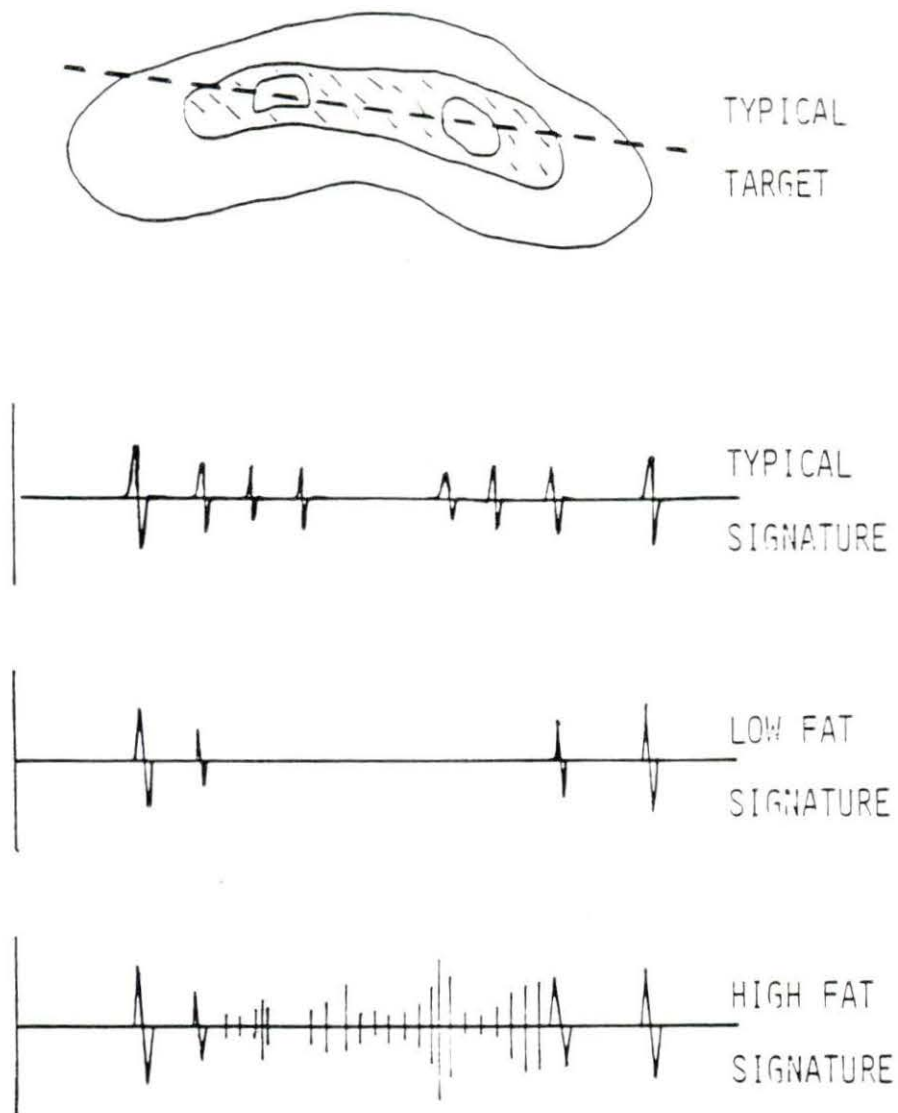


Figure 2.2 Ultrasound echo analysis from different interface boundaries (illustrated by Anselmo et al., 1987)

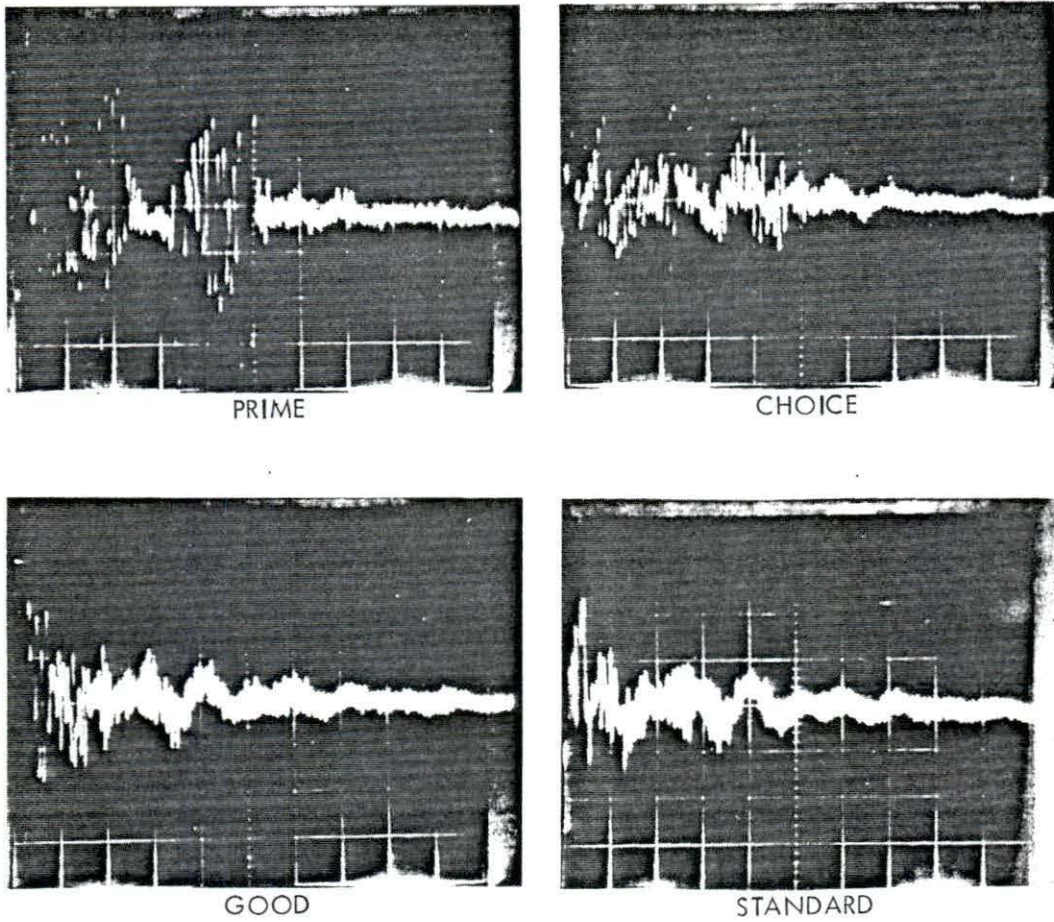


Figure 2.3 Analog A-mode signal from steak of different grades
(Anselmo et al., 1987)

with fibers, and this affects its acoustical properties (attenuation value). The attenuation coefficient value also depends on the orientation of muscle fibers and the angle at which the wave propagates into the muscle. For example, the attenuation in a direction parallel to the fibers is about twice that encountered when the wave is propagating perpendicular to the fibers (Christensen, 1988, page 53).

There are four major causes of the wave attenuation. First is the divergence of the waveform. The wavefront may not be planar but rather diverging. This leads to a dilution of the wave energy into an expanding cross-sectional area. Second is the elastic reflection at planar interfaces. Third is the elastic scattering from the irregular scatterers. Even within supposedly homogeneous tissue, there may be small, localized variations in acoustic properties which will lead to broad-angle scattering of the incident wave causing a reduction in forward power density. Fourth is the absorption of the wave energy. As the ultrasonic wave propagates into the tissue, a part of its original power is transferred into heat (Christensen, 1988, page 53 and Shung, 1987).

In previous studies, the acoustic attenuation coefficient has been successfully used as an indicator to distinguish an abnormal liver from a normal liver. In most experiments, it is found that the attenuation value is increased in a pathological liver. Kuc and Schwartz (1979) and Wilson et al.

(1984) found that a fatty liver has a greater attenuation value than a normal liver.

Relationship between Attenuation and Frequency

From the studies of attenuation in abnormal livers, it is known that the reflected signal is mainly influenced by small scatterers, so called Rayleigh scatterers (Narayana and Ophir, 1983; Round and Bates, 1987), irregular boundary effects (Kuc, 1980) and absorption (Merkulova, 1967). The relationship between the attenuation and the frequency is (Narayana and Ophir, 1983):

$$A(f) = A_0 f^n$$

where f = frequency

$A(f)$ = frequency dependent attenuation coefficient

A_0 = attenuation coefficient characteristic of the

tissue which is experimentally determined,

and n = power of frequency dependence of $A(f)$.

When the transmitted wave passes a small scatterer, the wave is reflected in all directions. It is known that the scattering increases with an increasing frequency. At the higher frequencies, the spectra are more distorted than at the lower frequencies. Thus, as an acoustic pulse propagates

through a volume of tissue with Rayleigh scatterers, it experiences a frequency dependent attenuation. Biological tissues have been observed to behave like distributed acoustic low-pass filters which attenuate higher frequencies more than lower frequencies. The components of an acoustic pulse propagating in that medium are attenuated to different degrees. These effects will disturb the pulseform.

Unlike the reflections from plane normal interfaces, the reflections from the irregular boundaries produce a time-limited spread-out response (noise). Thus, the reflected signal spectrum is also distorted by the irregular boundaries. The distortion is more complex in the inhomogeneous tissue; the spectral characteristics are changed by multiple reflections. Thus, when an ultrasonic pulse is reflected by a scattering body and an irregular boundary, the spectrum of the backscattered signal differs from the spectrum which was transmitted. It is no longer Gaussian shaped (Merkulova, 1967).

It is also found that during the propagation of the pulse in an attenuating medium, the spectral peak (center frequency) does not remain strictly constant. The spectral peak is shifted in the direction of the low frequency (Merkulova, 1967). Narayana and Ophir (1983) modeled fatty liver as normal liver tissue infiltrated by a large number of tiny fat globules that acted as Rayleigh scatterers. In a medium with

Rayleigh scatterers, it has been noticed that the peaks of the spectra are shifted towards lower frequencies (Narayana and Ophir, 1983). This downward shift due to the effect of acoustic attenuation was also noticed by Kuc et al. (1976).

The Least Squares Estimate of Attenuation Slope

A linear technique for measuring the attenuation coefficient ($A(f)$) and the slope of the attenuation coefficient (a) in liver was developed by Wilson et al. (1984). This linear technique was developed by dividing the A-mode backscattered signal into equally depth-spaced data segments and, then, processing the power spectra of each data segment. This linear technique was used since it was assumed that the amount of transmitted energy at a particular point in liver tissue is a linear function of the depth and the frequency. For this method, the power of frequency dependence of $A(f)$, n , in the attenuation coefficient equation on page 15 is equal to one. The attenuation coefficient ($A(f)$) is found by determining the linear slope of the magnitude of the power spectrum with respect to the depth in the tissue sample at a certain frequency within the bandwidth. The slope of the linear regression line of the attenuation coefficient ($A(f)$) with respect to the frequencies within the bandwidth gives the slope of the attenuation coefficient (a) of the tissue sample.

The frequency domain signal processing scheme was done using a method developed by Robinson (1979). To get a reasonably accurate picture of the spectrum of each data segment, each data segment is zero-padded. The power spectrum is calculated by finding the Discrete Fourier Transform (DFT) of the autocorrelated signal in each data segment. The phase effects between widely spaced echoes, which give ripples in spectral signals, are limited by multiplying the autocorrelation signals of each data segment with Hamming windows for the power spectrum to be smoothed.

CHAPTER 3. EXPERIMENTAL PROCEDURE

Data Acquisition System

The equipment used in these experiments included a Jameco 80286 IBM-compatible personal computer (Jameco Electronics, Belmont, CA, USA). This computer was equipped with a Heath Model SD5000 Digital Storage Oscilloscope system (Heath Co, Benton Harbor, MI, USA). This system can perform real-time sampling up to a rate of 20MHz and has an equivalent sampling rate from 50MHz up to 5GHz for 512 points. A Panametrics Pulser/Receiver, Model 5052PR, was used both to drive the input pulse voltage to the transducer and to receive the backscattered acoustic signal which was displayed on an analog and a digital storage oscilloscope. An ultrasound tank similar to the one used by Haumschild (Haumschild and Carlson, 1983) was used for angular measurements. Figure 3.1 shows the functional block diagram of the personal computer based data acquisition system (Chang, 1991). The ultrasound tank is displayed in Figure 3.2 (Amin, 1989).

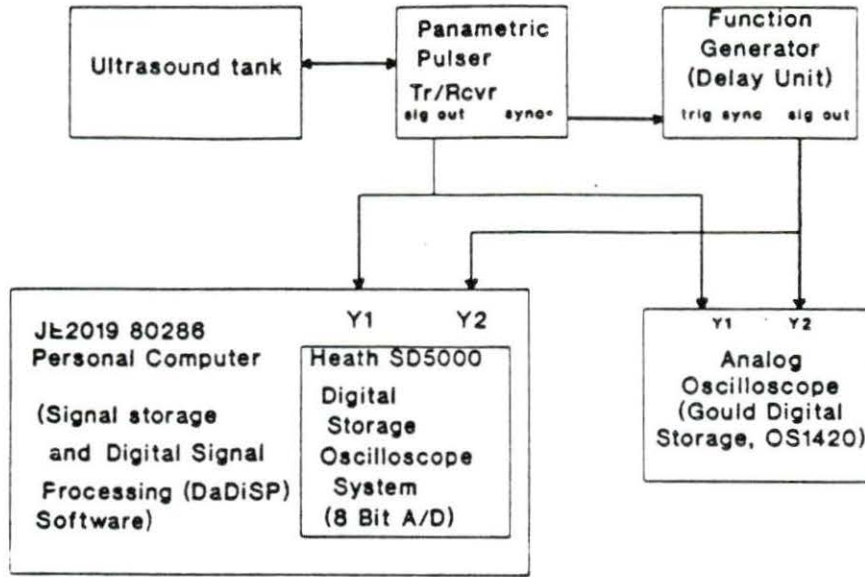


Figure 3.1 Functional block diagram of the PC-based data acquisition system (Chang, 1991)

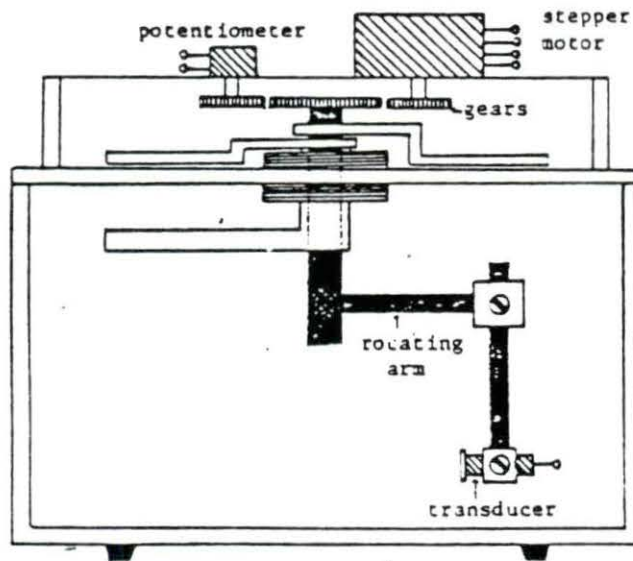


Figure 3.2 Ultrasound water tank (Amin, 1989)

Pulser/Receiver

The Panametrics Pulser/Receiver was used with a single transducer for the pulse-echo mode. This unit allowed control of the following variables:

- i) Energy (14-34 microJoules)
- ii) Damping (0-250 Ohms)
- iii) Pulse amplitude (140-270 Volts)
- iv) Gain/attenuation of receiver (0-63 dB)
- v) Highpass filter (0-1 MHz).

The controls on the Panametrics pulser were set to their optimum values with respect to the broadband transducer. These optimum values gave signals of least noise, good amplitude, and no baseline drift when displayed on the oscilloscope. The settings are shown in Table 3.1. They were not changed during the measurements of the samples.

Transducer

A broadband transducer was used in this experiment. It was a rectangular flexible contact Piezo Film Sensor (PFS) with a bandwidth 1.52 to 5.0 MHz. The center frequency of this transducer is 3.0 MHz. Figure 3.3(a) shows the impulse response of the transducer. The frequency response of the transducer is displayed in Figure 3.3(b). The impulse response of the transducer was found by reflecting the signal off a

Table 3.1 Parametric Pulser/Receiver Settings

Variable	Pulser settings
Repetition Rate	Max
Energy	Max
Damping	5
Attenuation	4dB
Gain	40dB
High Pass Filter	0.3MHz

half-inch thick piece of flat smooth plexiglass plate placed perpendicular to the path of the sound beam in a water bath.

Instead of duplicating its electrical input voltage (sharp pulse), the transducer has an exponentially decaying sinusoidal pressure waveform output. The rate of the decay is inversely proportional to the quality factor (Q) of the transducer. The equation of the rate of the decay (γ) in terms of Q is:

$$\gamma = \frac{2 \pi f_1}{Q} = \frac{w_1}{Q}$$

where γ = decay rate of the pressure waveform of the transducer

f_1 = frequency of resonance in Hz

w_1 = angular frequency of resonance in rad/s

and Q = quality factor of transducer.

A low Q value increases the decay rate of the pressure wave radiation. The envelope of the pressure wave radiating from a transducer with a given Q is:

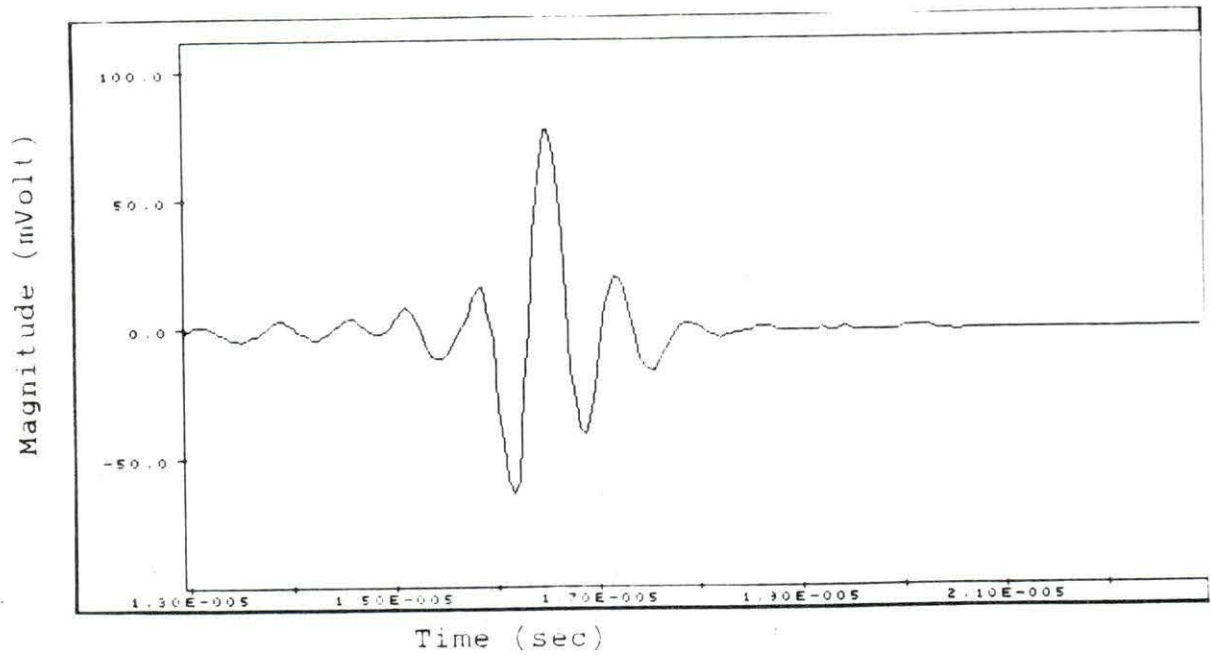
$$p(t) = p_0 e^{-(\gamma/2)t}$$

where p_0 = pressure waveform at $t=0$

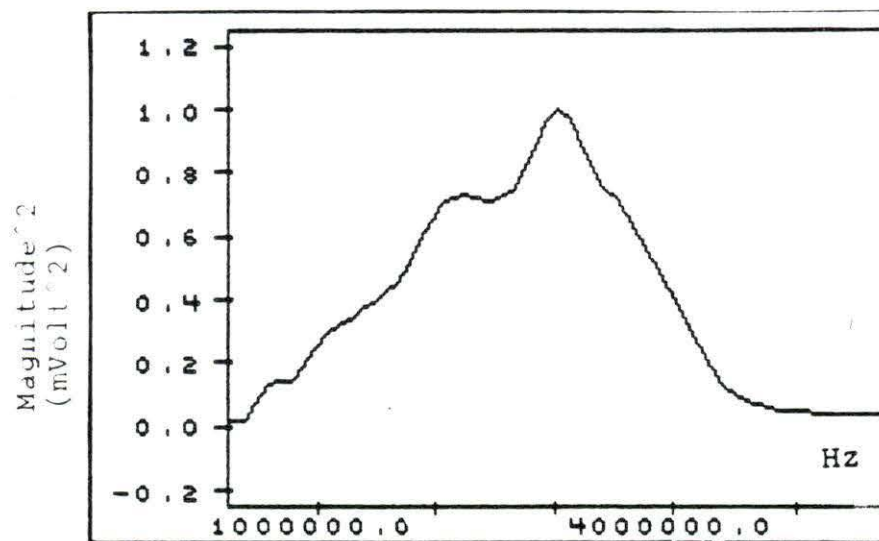
p = pressure waveform at t

and γ = decay rate of pressure waveform.

If the exponential decline of the pressure waveform of the transducer can be shortened, the axial resolution can be improved. Thus, a low Q value of the transducer is desirable so that the transducer will radiate a short pressure waveform. A shorter transmitted pulse will allow the measurement of the spatial or axial resolution of the reflecting borders. Thus, a narrow impulse response received from the transducer will have a broad bandwidth frequency response which will give better resolution.



(a)



(b)

Figure 3.3 Characteristic of the transducer (a) Impulse response (b) Frequency response

Preparation of the Beef Samples

Longissimus dorsi muscle samples were taken between the 12th and 13th ribs. They were packed in air-evacuated plastic bags and then graded according to the USDA standards by qualified meat graders. These samples were categorized into one of four USDA standard classifications - Prime, Choice, Good, and Standard(Select)- by subjectively observing the degree of visible marbling. The packages are kept frozen until they could be tested. They were then cut into smaller pieces before taking measurements. The samples were carefully cut so that the front surface formed a curvature about 10 cm in radius as shown in Figure 3.4 (Chang, 1991). This curved front surface was cut as flat as possible; this allows the front surface to be kept perpendicular to the transducer. This allows the ultrasonic waveform to propagate perpendicular to muscle fibers of the sample. The thickness and the depth of the samples were about 4 cm. Figure 3.5 (Chang, 1991) shows the anatomical references of the longissimus dorsi muscle, the white lines are the approximate boundaries of the samples.

The samples were individually placed at the bottom of the water tank which contained slightly salted water. The water temperature was regulated at 35° C.

Precautions Taken During Measurements

Some of the precautions taken during scanning of the samples are listed below.

- * Water in the tank was maintained at 35° C.
- * Data samples and transducer face were freed as much as possible from air bubbles in the water.
- * The end of the A-mode signal was checked on the analog oscilloscope.
- * The water was not moving when the measurements were taken.

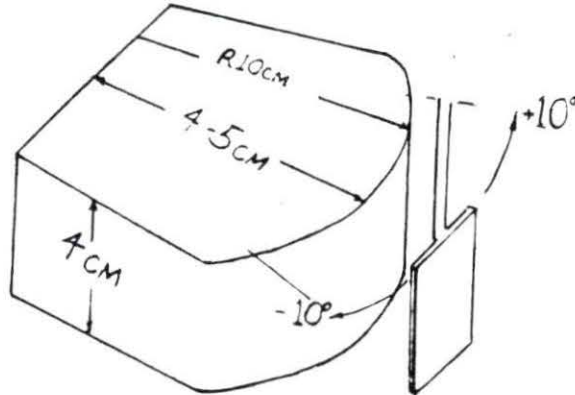


Figure 3.4 The sample cut from the longissimus dorsi positioned with the rectangular-shaped broadband transducer for data sampling (Chang, 1991)

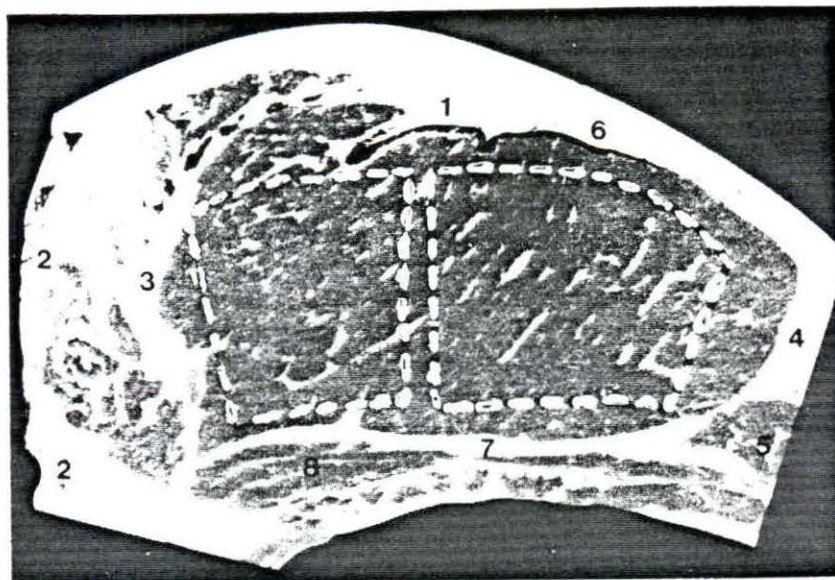


Figure 3.5 Anatomical references of the 12th-13th ribeye steaks. (1) Acorn fat depot, (2) spine, (3) medial end, (4) lateral end, (5) longissimus costarum, (6) proximal border, (7) distal border, and (8) intercostal muscle. Dotted line marks how the samples were cut (Chang, 1991)

Sampling the A-Mode Signals

The pulse-echo signal of a sample was received back at the broadband transducer which was placed approximately 2 cm from the tissue sample. The backscattered signal measurements were taken from a line of sight from $+10^{\circ}$ to -10° with an increment of 2.5° . Thus, there were nine lines of sight or angles for each sample. To avoid the aliasing effect, the

backscattered signal had to be sampled according to the Nyquist rate. Thus, the backscattered signal had to be digitized at a sampling rate that was at least twice the maximum frequency component in the analog signal (Proakis and Manolakis, 1988, page 25). The backscattered signals were digitized or sampled at a rate of 20 MHz which is greater than the maximum frequency of 5 MHz. Consequently, the pulse echo signal (backscattered signal) could be reconstructed from the digitized data without aliasing.

Windowing the A-Mode Signal

The A-mode backscattered signal was digitized by the digital storage oscilloscope at the sampling rate of 20 MHz. Although 1475 points of data were recorded, only 1024 points of data were used in the experiment. These 1024 points covered 39.4 mm of depth into the meat samples. This A-mode backscattered signal was divided into a minimum of nine overlapping segments using 256-point rectangular windows. Each window corresponded to 9.86 mm, assuming the average velocity of the sound was 1540 m/s. It was necessary to eliminate the first 100 to 150 points of the A-mode backscattered signal to avoid the big reflection caused by the water-tissue boundary. Thus, the remaining A-mode signal was divided into small segments which corresponded to the reflections due to the

irregular interfaces within the tissue encountered along the acoustic beam path.

Frequency Domain Processing

In this experiment, the attenuation coefficient was computed in the frequency domain. Power spectra were calculated using a series of short segments of data, chosen to be short enough that the attenuation within the window could be assumed negligible, but long enough to adequately sample the spectrum. For better resolution, each of the 256-point windowed segments in one line of sight A-mode signal was extended by zero padding to make a 512-point data segment.

The power spectrum of each 512-point data segment was obtained by squaring the magnitude of its Discrete Fourier Transform (DFT), using the Radix-2 Fast Fourier transform (FFT) algorithm program which is shown in Appendix C. However, this power spectrum has many ripples in magnitude which are not directly related to the local tissue characteristic, but are merely due to phase effects between widely spaced echoes. It was assumed that each windowed tissue volume contained random scatterers and that the raw spectrum incorporated perturbations due to interference between scatterers from adjacent window segments. Thus, to reduce the phase effects between widely spaced echoes which give ripples (distortion) in the spectrum, windowing in the autocorrelation domain was

necessary (Robinson, 1979). In other words, the spectra were smoothed by windowing the autocorrelation signal with a 256-point Hamming window. This 256-point Hamming window in the autocorrelation domain was suitable for removing the effects of approximately 4.89 mm or greater spaced echoes and leaving only the contributions from closely spaced echoes.

The Quick-BASIC program used to calculate the autocorrelation of the windowed segment signals is shown in the Appendix C. The autocorrelation algorithm is:

$$r(m) = \frac{1}{2N} \sum_{n=-N}^N x(n)x(n+m)$$

where $r(m)$ = autocorrelation of Discrete Time (DT)
 signal $x(n)$ with lagging m
 $x(n)$ = DT signal
 $x(n+m)$ = DT signal $x(n)$ with lagging m
 and $N = 512$.

Multiplying the autocorrelation of the windowed segment with a 256-point Hamming window eliminated the phase effects caused by multiple reflections which were separated in space by 4.89 mm or more. The Radix-2 FFT Quick-BASIC program was run to determine the power spectrum of the filtered autocorrelate data signal.

Mean Square Linear Regression Method

At each frequency within the transducer bandwidth, the attenuation coefficient was computed as a slope of the least squares regression of the smoothed log-power spectra with respect to depth of the 512-point data segments in one line of sight A-mode signal. Let the smoothed log-power spectra at frequency f and depth d_i in one line of sight be $P(d_i, f)$. The attenuation coefficient $A(f)$ at frequency f is the slope of a linear fit of P as a function of depth and is given by the expression for the slope of the regression line as:

$$A(f) = \frac{\sum_i P(d_i, f) (d_i - d)}{2 \sum_i (d_i - d)^2}$$

where $A(f)$ = attenuation coefficient

d_i = depth in tissue

and d = mean depth in tissue.

To examine the attenuation coefficient $A(f)$ in the meat sample, the smoothed power spectra was extracted only within the average bandwidth, 1.5 MHz to 5 MHz.

Next, a least squares regression was performed on the attenuation coefficient $A(f)$ as a function of frequency over the bandwidth. The slope of the attenuation coefficient for one line of sight is:

$$a = \frac{\sum_i A(f_i) (f_i - f)}{\sum_i (f_i - f)^2}$$

where a = slope of the attenuation coefficient

$A(f_i)$ = attenuation coefficient

f_i = frequency over the bandwidth

and f = mean frequency over the bandwidth.

Then, the slopes of the attenuation coefficient from different lines of sight were averaged.

Summary of Experimental Steps

The steps in processing the backscattered signals are shown below. They are summarized in Figure 3.6.

- * Organize the data into overlapping 128-point segments or segment the data with 256-point rectangular windows that overlap at the center (128th point).
- * Zero-pad each segment (512-point).
- * Compute the power spectra of each segment by using Radix-2.
- * Compute the attenuation coefficient, $A(f)$, at each frequency over the bandwidth for each segment in one line of sight using least squares method.

- * Compute the slope of the attenuation coefficient with respect to frequency within the bandwidth.
- * Average the slopes of the attenuation coefficient, a , from all lines of sight for a given tissue sample.

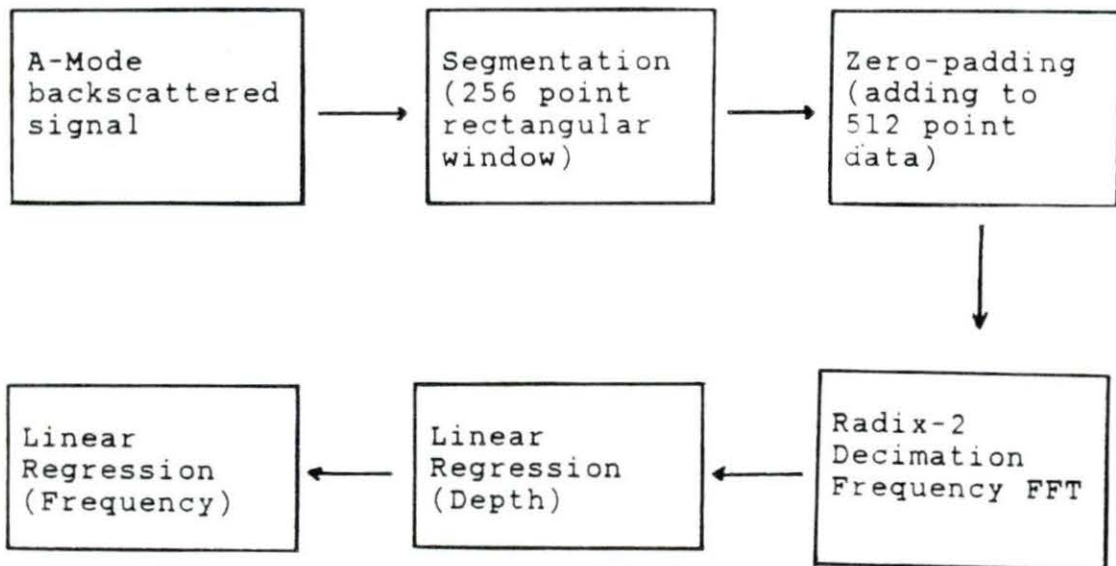


Figure 3.6 Block diagram of the method used to process the raw backscattered signal

CHAPTER 4 RESULTS AND DISCUSSION

Samples were cut from different parts of the longissimus dorsi muscles between the 12th and the 13th ribs. The data were taken from ten samples from four different longissimus dorsi muscles which had been graded prime, choice(+), choice and select(-). The locations of the 10 samples in the longissimus dorsi muscles are shown in Table 4.1. Table 4.1 also lists the fat percentage obtained from the ether extraction analysis and the mean value of the slope of the attenuation coefficient obtained from each sample. To illustrate the process used in obtaining the slope of the attenuation coefficient, the following section will show the steps and results for the 9.18% fat sample.

Signal Processing in 9.18% Fat Sample

The A-mode backscattered signal received at the transducer was sampled by a digital storage oscilloscope at a sampling rate of 20 MHz. Figure 4.1 displays a real-time A-mode backscattered signal at one line of sight (0° angle) from a 9.18% fat sample. This A-mode signal displays the amplitudes

Table 4.1 The location of the samples in the longissimus muscle, the percentage fat and the slope of the attenuation coefficient

Grade of ribeye	Location on the Longissimus muscle	Percentage of fat (chemical test)	Mean slope of the attenuation coefficient (all lines of sight)
Prime Prime	Lateral end Medial end	10.88 9.18	2.30 2.27
Choice (+)	Lateral end at proximal border	5.20	1.95
Choice (+)	Lateral end below acorn fat depot	7.19	1.75
Choice (+)	Medial end below acorn fat depot	9.45	1.98
Choice (+)	Medial end at distal border	8.85	1.98
Choice Choice	Lateral end Medial end	3.56 1.52	1.39 0.83
Select (-)	Lateral end at distal border	2.74	1.32
Select (-)	Medial end below acorn fat depot	2.28	1.14

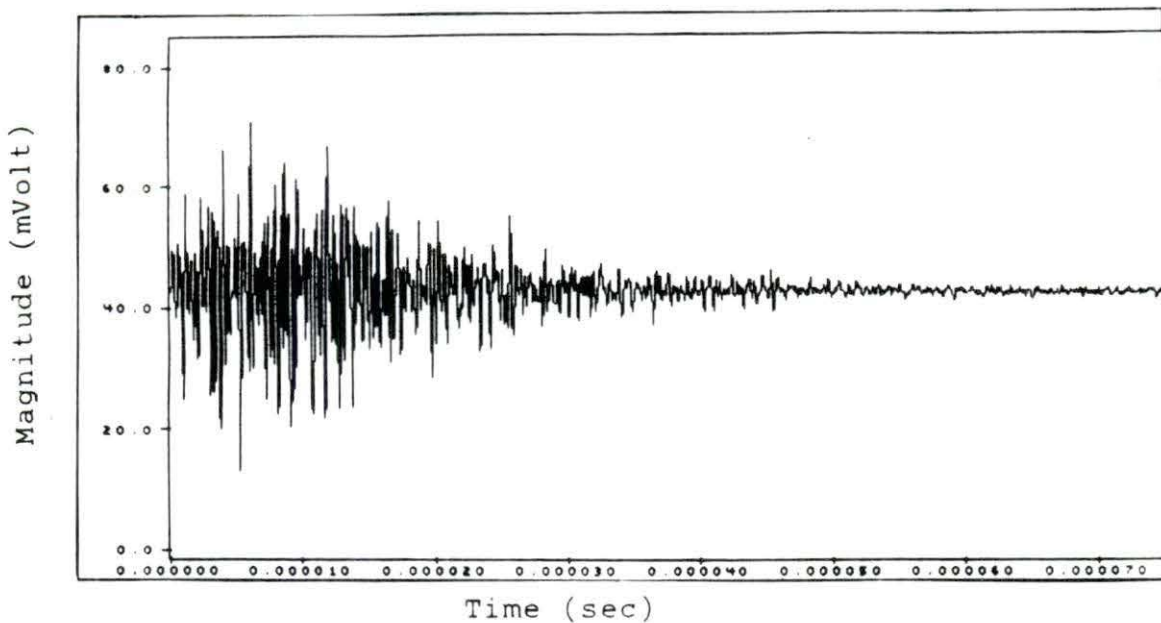


Figure 4.1 Backscattered signal sampled at 20 MHz from one line of sight (0° angle)

of the signal reflected from the irregular boundaries and Rayleigh scatterers in the meat sample. By dividing the backscattered into smaller, equally spaced segments, the characteristic of the meat sample within a particular depth can be observed more carefully. The segmentation of the backscattered signal with a 256-point rectangular window provides the tissue characteristics of the meat within approximately 1 cm depth. Figure 4.2 shows the backscattered signal divided into 256-point data segments.

Figure 4.3 illustrates the result of expanding a 256-point data segment to a 512-point data segment by zero-padding. The zero padding provides sufficient detail of the

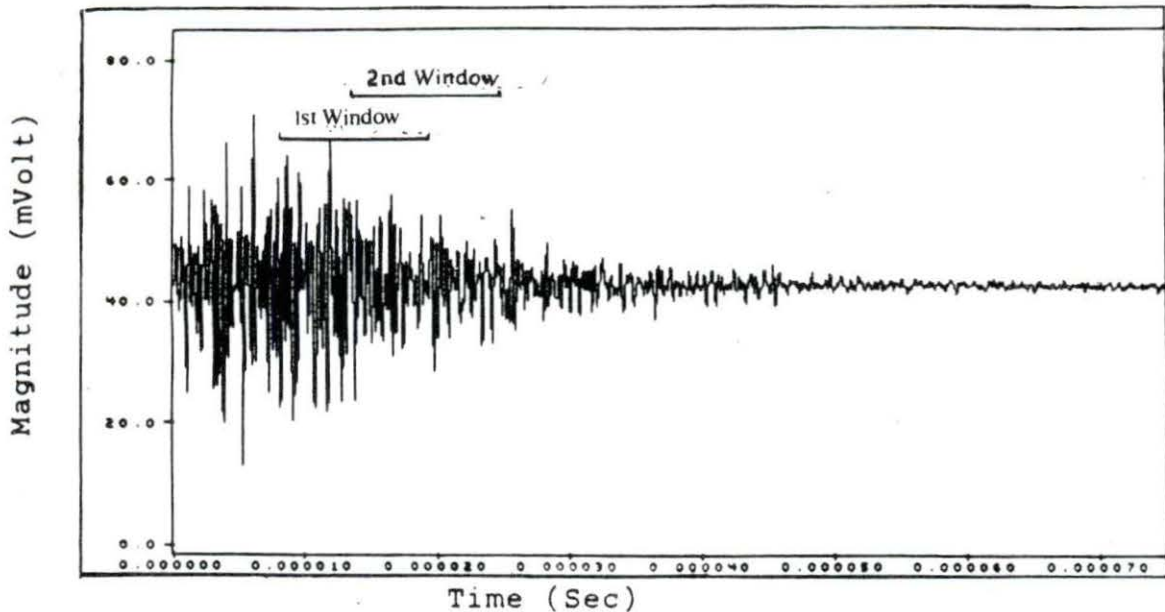


Figure 4.2 Backscattered signal divided into 256-point data segments

power spectra of 256-point data segment. The power spectrum and the log-power spectrum of this expanded data segment are shown in Figure 4.4(a) and (b), respectively. These power spectra have many ripples in their magnitudes. These ripples are not a characteristic function of the tissue sample; they are phase effects due to multiple reflections of widely spaced echoes. Figure 4.5 (c) shows the result of multiplying the autocorrelation of the data segment, Figure 4.5 (a), with 256-point Hamming window, Figure 4.5 (b). Figure 4.6 (a) and (b) illustrate the power spectrum and the log-power spectrum of the autocorrelation signal after the smoothing process.

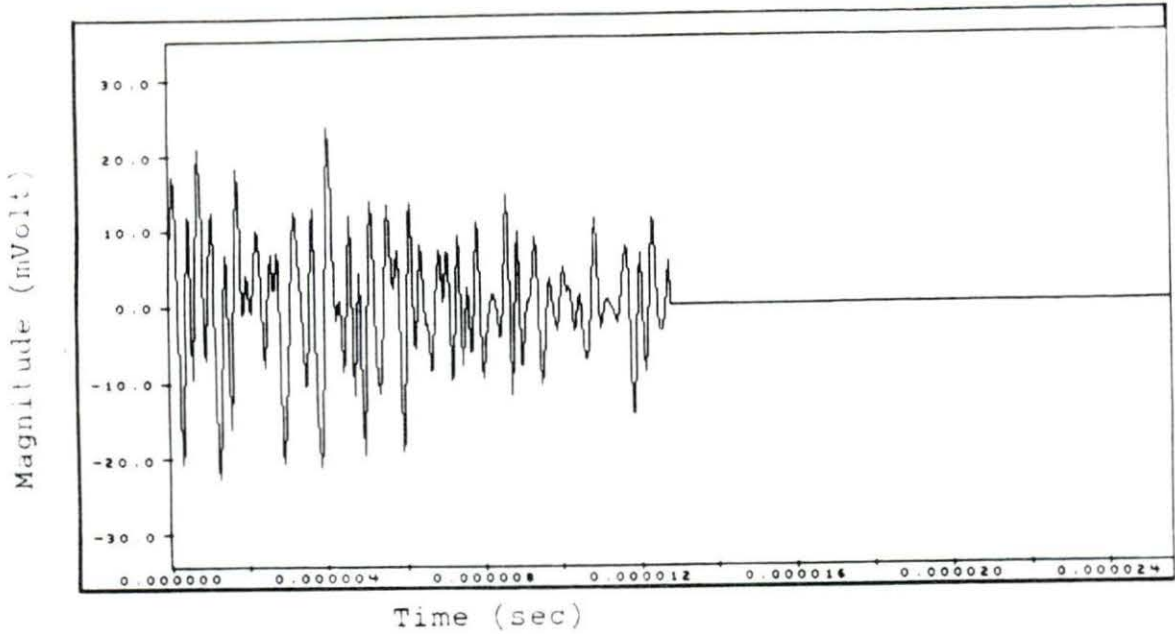


Figure 4.3 Result of zero-padding the first 256-point window segment

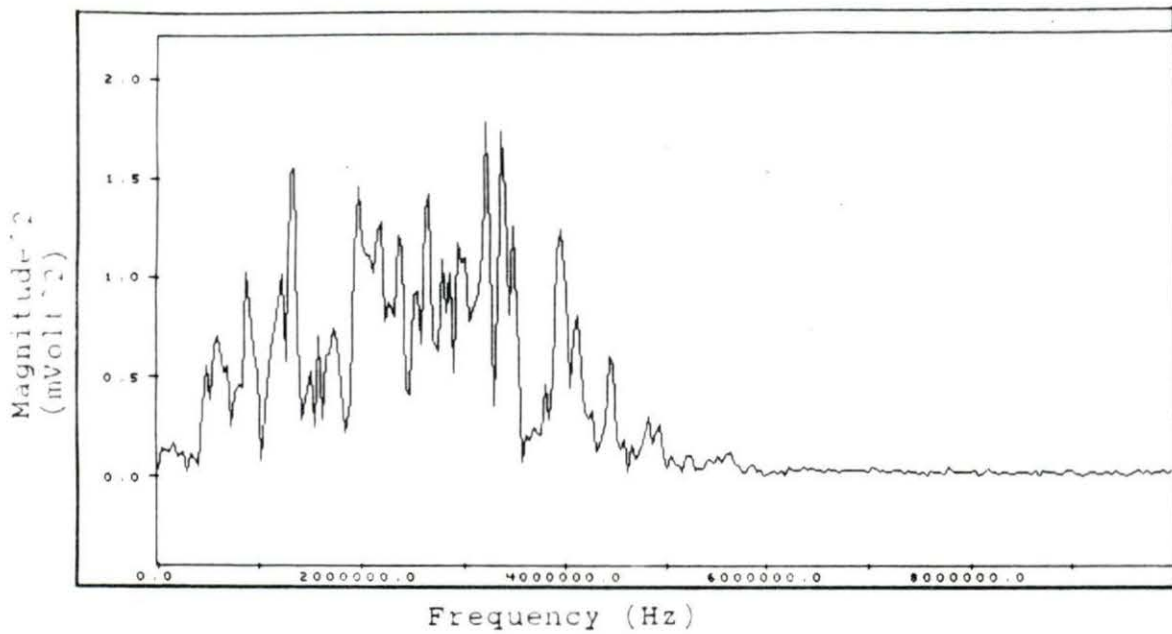


Figure 4.4 The result of FFT without smoothing process (a) power spectrum of a 512-point data segment

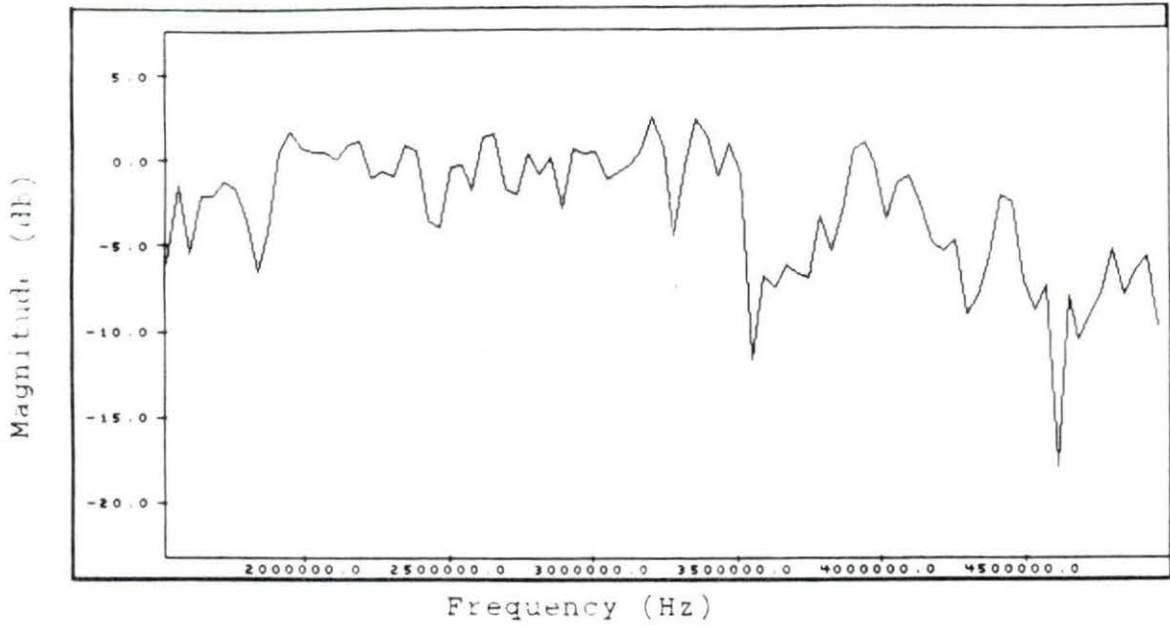


Figure 4.4 (continued) (b) log power spectrum

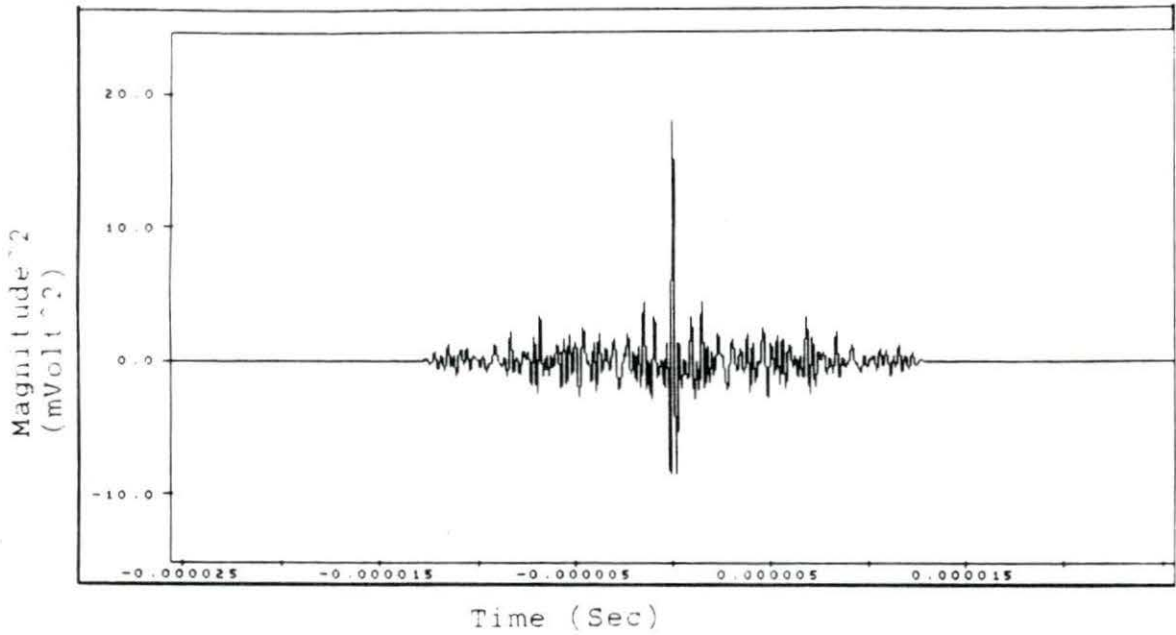
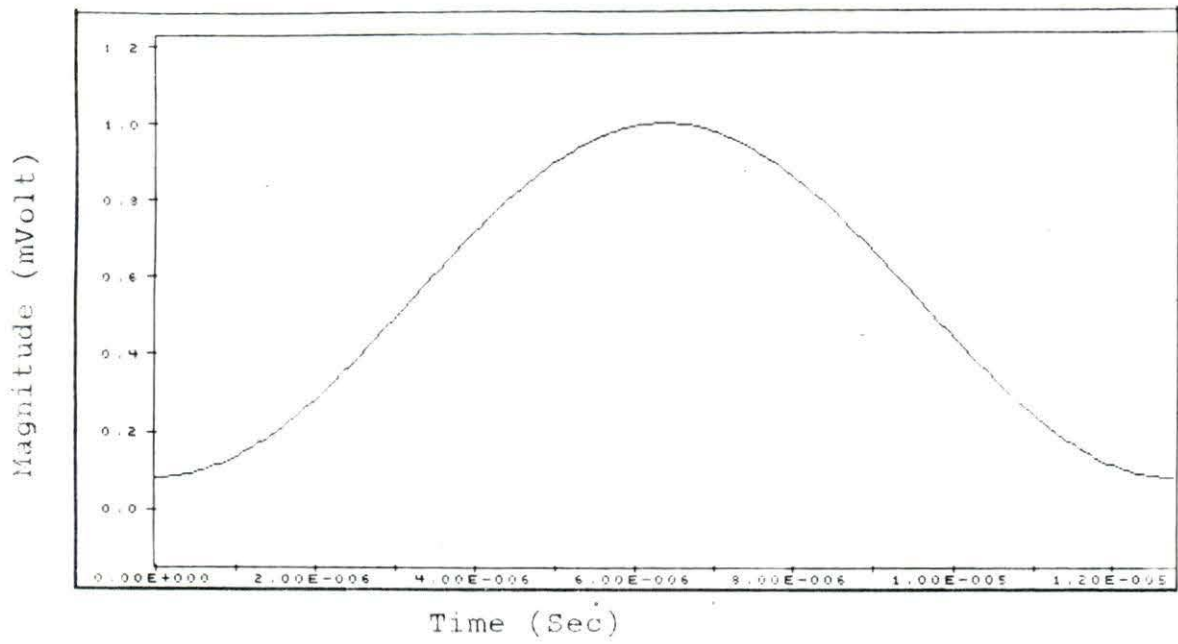
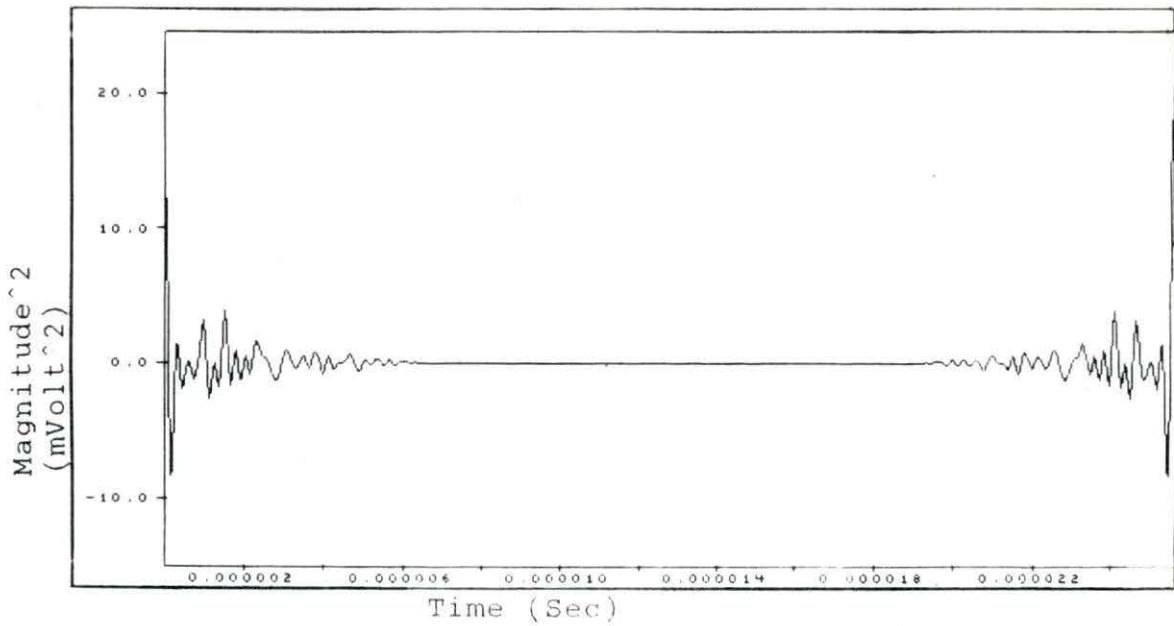


Figure 4.5 Smoothing process (a) autocorrelation of a back-scattered signal from a 512-point window segment

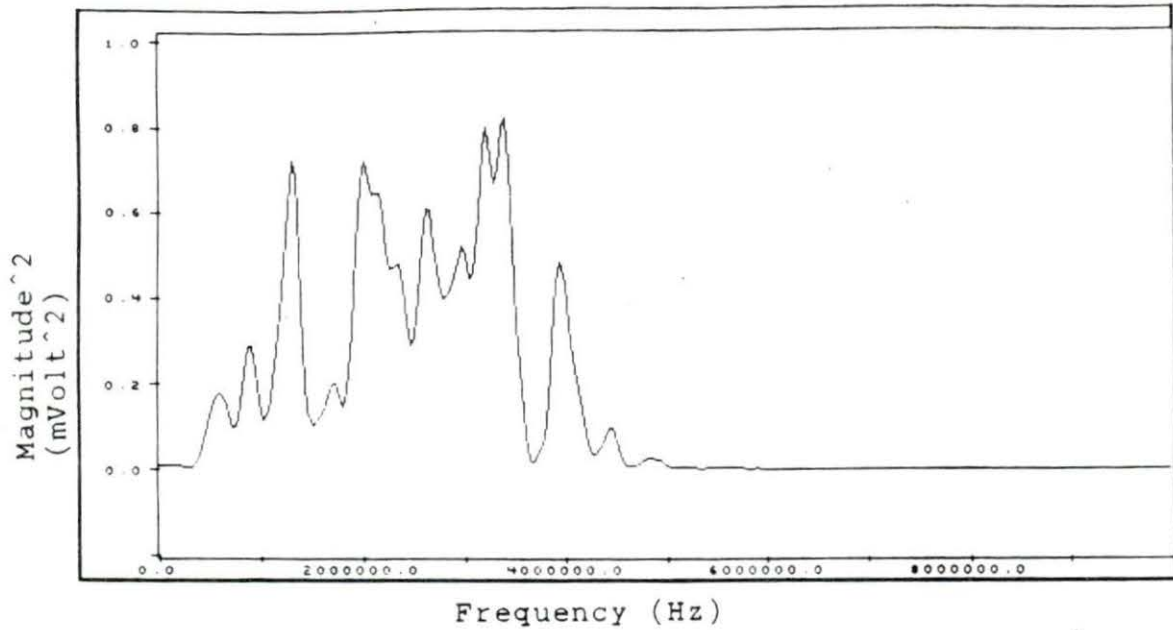


(b)

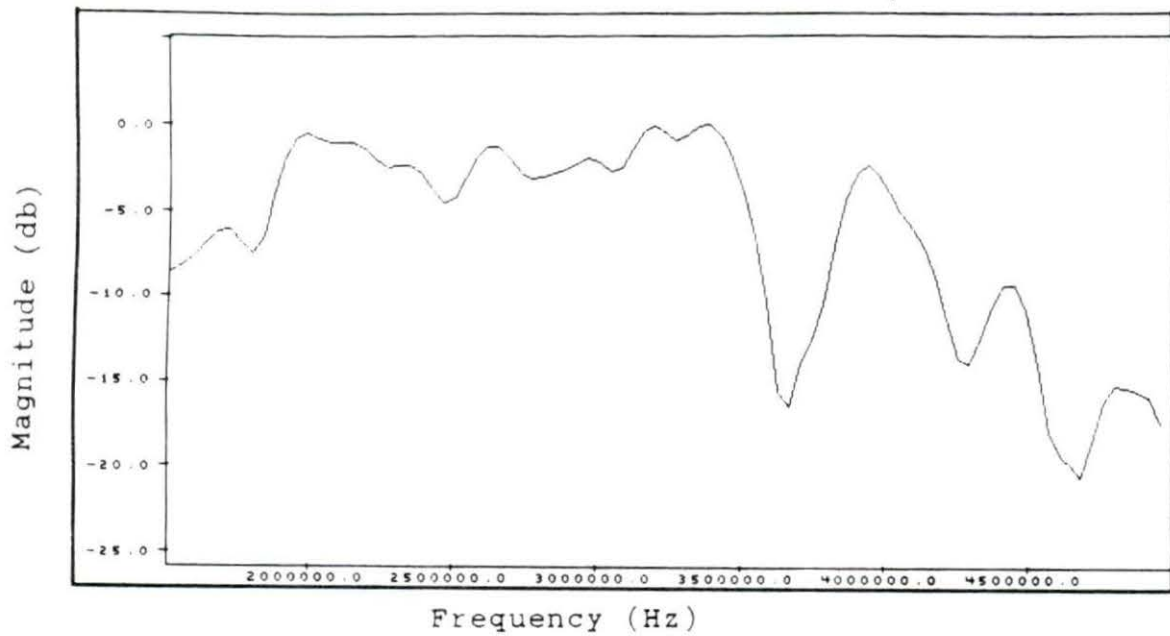


(c)

Figure 4.5 (continued) (b) 256-point Hamming window (c) the autocorrelation signal filtered by 256-point Hamming window



(a)



(b)

Figure 4.6 The result of FFT after smoothing process (a) power spectrum of a 512-point data segment (b) log-power spectrum

The magnitudes of the power spectra at various depths in the tissue sample along one line of sight (0° angle) are shown in Table 4.2. The linear model for the data in Table 4.2 can be estimated using the least squares linear regression method:

Table 4.2 The spectral magnitude from 11 windows at a frequency 1.52 MHz. These data were recorded at 0° angle line of sight from a sample with 9.18% fat

Depth (cm)	Window	Spectrum magnitude at 1.52 MHz (mVolt ²)
0.7623	1	1.03
0.9510	2	0.72
1.1396	3	0.97
1.3283	4	1.56
1.5169	5	0.99
1.7056	6	2.02
1.8942	7	0.25
2.0829	8	0.06
2.2715	9	0.08
2.4602	10	0.06
2.6488	11	0.01

$$y = b_0 + b_1x$$

where b_1 is the slope of the linear regression line. This is the attenuation coefficient $A(f)$ with respect to depth at a certain frequency within the bandwidth. The attenuation coefficient can be calculated as:

$$A(f) = \frac{S_{xy}}{S_{xx}}$$

where

$$S_{xx} = \sum_i (x_i - \bar{x})^2 = \sum_i (x_i)^2 - ((\sum_i x_i)^2/n)$$

$$S_{xy} = \sum_i (x_i - \bar{x})(y_i - \bar{y}) = \sum_i x_i y_i - ((\sum_i x_i)(\sum_i y_i)/n)$$

x_i = independent variables
 \bar{x} = mean value of independent variables
 y_i = dependent variables
 \bar{y} = mean value of dependent variables
and n = number of data.

Figure 4.7 shows the linear fit of a smoothed log-power spectrum with respect to the depth within the sample described in Table 4.2.

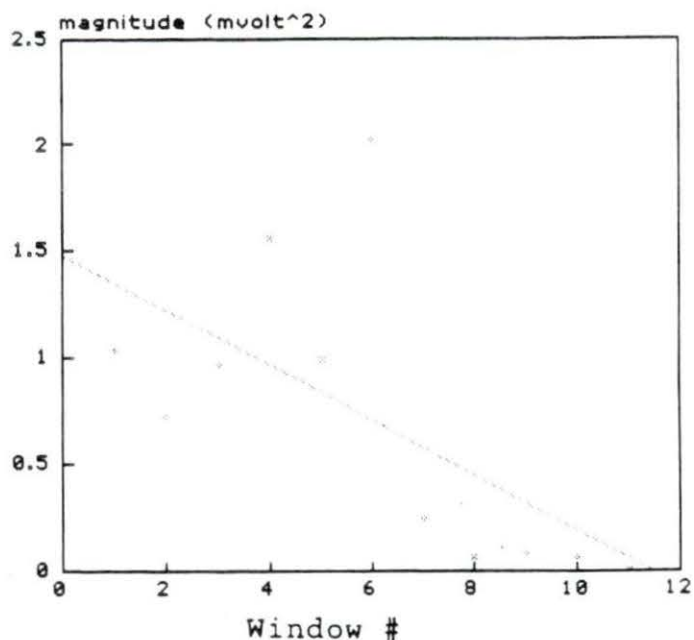


Figure 4.7 The linear regression of the data from Table 4.2

The slope of the attenuation coefficient (α) of the tissue sample was computed by finding the slope of the linear regression of the attenuation coefficient, $A(f)$, with respect to the frequencies within the bandwidth as shown in Figure 4.8. The best fit of the linear model was also determined by the least squares method as mentioned above, the slope of the attenuation coefficient, (α), is 2.86 dB/cm-MHz. The same process was then followed for the other lines of sight for each sample and the slopes of the attenuation coefficients were averaged. For the 9.18% fat sample this average value was 2.27 dB/cm-MHz (Table 4.1).

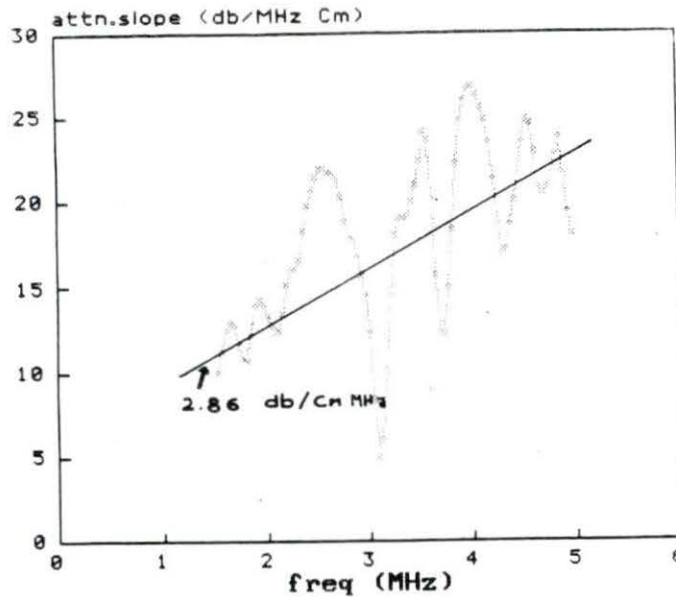


Figure 4.8 The slope of the attenuation coefficient of a 9.18% fat sample at 0° line of sight within the bandwidth 1.52 - 5.00 MHz

Ether Extraction Analysis (Chemical Test)

The ether extraction analysis was performed by the Meat Laboratory of Animal Science Department at Iowa State University. Table 4.1 indicates that the fat percentage of the ten samples increased according to the grades of the samples, from Select(-) to Prime. The detailed procedures of this ether extraction analysis are in the Appendix B.

Slope of the Attenuation Coefficient of Each Sample

The mean slopes of the attenuation coefficients of the backscattered signals from the ten samples ranged from 0.83 dB/cm-MHz to 2.30 dB/cm-MHz. The mean slope for the attenuation coefficient for each data sample was determined by averaging the values of the slopes of the attenuation coefficients from the nine different lines of sight (angles). These results support the hypothesis that the slope of the attenuation coefficient increases linearly as the fat percentage increases. This is shown in Figure 4.9. The slope of the linear fitting of the mean slope of the attenuation coefficient values as a function of the fat percentage is 0.1349 with the p-value equal to 0.0001. (The SAS program and the results of the slope calculation can be found in Appendix D.) Thus, the mean slope of the attenuation coefficient value can be used as one of the parameters to estimate the fat percentage in a meat sample. Tables A1 to A10 (Appendix A) show the values of the slopes of the attenuation coefficients of the samples used in this experiment. The mean slope of the attenuation coefficient increases as the mean of the fat percentage increases from Select(-) to Prime as shown in Table 4.3.

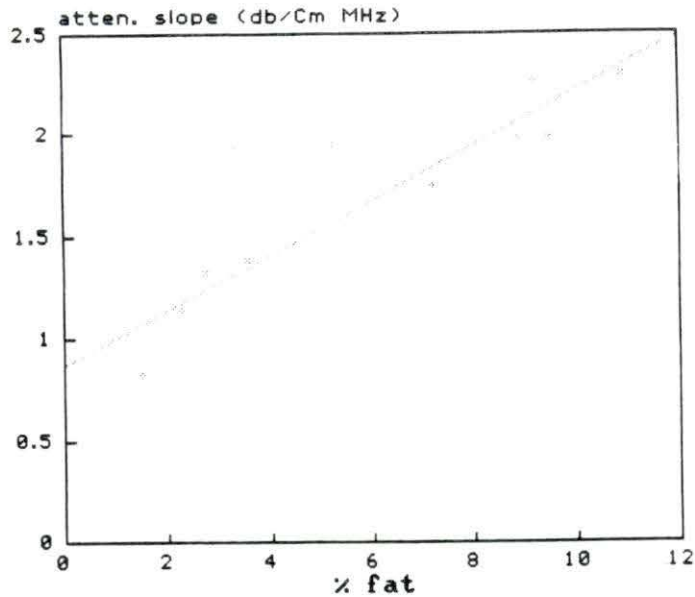


Figure 4.9 The linear fitting of the slope of the attenuation coefficient as a function of % fat

The statistical test of the significance of the difference in values of the data samples was done using the SAS program from the WYLBUR system (Appendix D). The hypothesis that is used in this test is that the mean of the slopes of the attenuation coefficient from nine lines of sight in a particular data sample is equal to the mean of the slopes of the attenuation coefficient value of each of the other data samples. The result of the SAS program gave the p-value that determined whether the differences are great enough to reject the hypothesis. The resulting p-values are listed in Table 4.4. The hypothesis used in Table 4.4 assumes that the mean

Table 4.3 The slope of the attenuation coefficient measured from 9 different angles and the percentage of fat of 10 samples

Fat Percentage	-10	-7.5	-5	-2.5	0	2.5	5	7.5	10	Mean of a	Standard Deviation
10.88	2.35	2.03	2.36	1.90	2.27	1.51	2.85	2.41	3.03	2.30	0.46
9.45	1.66	2.63	1.95	1.87	2.15	2.21	1.29	1.71	2.39	1.98	0.41
9.18	2.47	1.89	3.30	1.62	2.86	2.40	2.17	2.17	1.51	2.27	0.57
8.85	1.57	1.45	1.70	2.46	1.88	2.94	1.68	2.18	1.98	1.98	0.48
7.19	1.66	1.88	1.86	2.03	1.71	1.16	1.86	1.91	1.71	1.75	0.25
5.20	X	X	1.62	1.62	2.67	1.63	1.42	2.75	1.96	1.95	0.54
3.56	1.55	1.11	X	1.74	1.16	X	1.16	1.18	1.83	1.39	0.31
2.74	1.01	1.26	1.64	1.79	1.82	0.57	0.85	1.20	1.75	1.32	0.45
2.28	0.99	1.12	0.86	1.17	0.82	0.80	X	1.37	1.97	1.14	0.39
1.52	0.59	0.36	1.30	0.51	0.99	0.33	1.11	1.18	1.10	0.83	0.38

Table 4.4 The p-value of samples

Hypothesis: $\mu_A = \mu_B$

where μ_i = mean value of slope of the attenuation coefficient of sample i

A \ B	1.52	2.28	2.74	3.56	5.20	7.19	8.85	9.18	9.45	10.88
1.52		0.1500	0.0192	0.0127	0.0001	0.0001	0.0001	0.0001	0.0001	0.0001
2.28	0.1500		0.3879	0.2658	0.0005	0.0047	0.0001	0.0001	0.0001	0.0001
2.74	0.0192	0.3879		0.7543	0.0052	0.0384	0.0019	0.0001	0.0018	0.0001
3.56	0.0127	0.2658	0.7543		0.0179	0.1017	0.0085	0.0002	0.0083	0.0001
5.20	0.0001	0.0005	0.0052	0.0179		0.3658	0.8938	0.1580	0.8859	0.1165
7.19	0.0001	0.0047	0.0384	0.1017	0.3658		0.2680	0.0147	0.2635	0.0093
8.85	0.0001	0.0001	0.0019	0.0085	0.8938	0.2680		0.1713	0.9914	0.1242
9.18	0.0001	0.0001	0.0001	0.0002	0.1580	0.0147	0.1713		0.1746	0.8629
9.45	0.0001	0.0001	0.0018	0.0083	0.8859	0.2635	0.9914	0.1746		0.1268
10.88	0.0001	0.0001	0.0001	0.0001	0.1165	0.0093	0.1242	0.8629	0.1268	

value of the slope of the attenuation coefficient of sample A equals the mean value of the slope of the attenuation coefficient of sample B. For p-values below 0.01, the hypothesis is rejected which means the difference in values for those two samples is statistically significant.

Observing the p-values of the comparison of the means of the slope of the attenuation coefficient from Table 4.4, the samples can be grouped into seven groups as shown in Table 4.5. The p-values obtained by comparing the 1.52% fat percentage sample and the 2.28%, 2.74% and 3.56% fat percentage samples are 0.1500, 0.0192, and 0.0127, respectively. These p-values are greater than 0.01 which indicates that the hypothesis can not be rejected. Thus, the mean of the slopes of the attenuation coefficient of the sample with 1.52% fat is not significantly different from the mean of the slopes of the attenuation coefficient of samples with 2.28%, 2.74%, and 3.56% fat. The grouping of the samples according to means of the slope of the attenuation coefficient can be simplified into three categories. Groups 1 and 2 shown in Table 4.5 can be grouped with group 3. Groups 4 and 6 can be grouped with group 7. Thus, these categories are: the slope of the attenuation coefficient ranges from 1.39 - 2.30 dB/cm-MHz (group I), 1.32 - 1.98 dB/cm-MHz (group II), and 0.83 - 1.75 dB/cm-MHz (group III).

Table 4.5 Grouping of samples with no significant difference in the mean slopes of the attenuation coefficients

Sample with % fat (%)	a (dB/cm-MHz)	Group
1.52, 2.28, 2.74, 3.56	0.83, 1.14, 1.32, 1.39	1
1.52, 2.28, 2.74, 3.56, 7.19	0.83, 1.14, 1.32, 1.39, 1.75	2
1.52, 2.28, 2.74, 3.56, 5.20, 7.19	0.83, 1.14, 1.32, 1.39, 1.95, 1.75	3
5.20, 7.19, 8.85, 9.18, 9.45, 10.88	1.95, 1.75, 1.98, 2.27, 1.98, 2.30	4
2.74, 3.56, 5.20, 7.19, 8.85, 9.18, 9.45	1.32, 1.39, 1.95, 1.75, 1.98, 2.27, 1.98	5
5.20, 7.19, 8.85, 9.18, 9.45, 10.88	1.95, 1.75, 1.98, 2.27, 1.98, 2.30	6
3.56, 5.20, 7.19, 8.85, 9.18, 9.45, 10.88	1.39, 1.95, 1.75, 1.98, 2.27, 1.98, 2.30	7

Attenuation Slope of the Longissimus Dorsi Muscle Sample

If the samples are categorized according to meat grade, the data samples can be grouped into four different categories. Table 4.1 gives the grades, the locations of the samples, information about the mean of the slopes of the attenuation coefficient, and the percentage of fat of the samples.

Using the SAS program from the Wylbur system (Appendix D), each of the samples was tested to determine if the mean

slopes of the attenuation coefficient of two samples based on grade were different. Thus, the hypothesis used in this test was that the mean values of the slopes of the attenuation coefficient of the two samples are the same. The results of these tests determine the p-value which indicates the probability of making an error if the hypothesis is rejected. Table 4.6 shows the p-values. From Table 4.6, it can be concluded that there is no difference between the mean slopes of the attenuation coefficient of samples graded Choice and Select(-) since the p-value is 0.4359. However, the results show that there are differences between Prime and Choice(+), Prime and Choice, Prime and Select(-), Choice(+) and Choice, and Choice(+) and Select(-) since the p-values are 0.0053, 0.0001, 0.0001, 0.0001, and 0.0001, respectively.

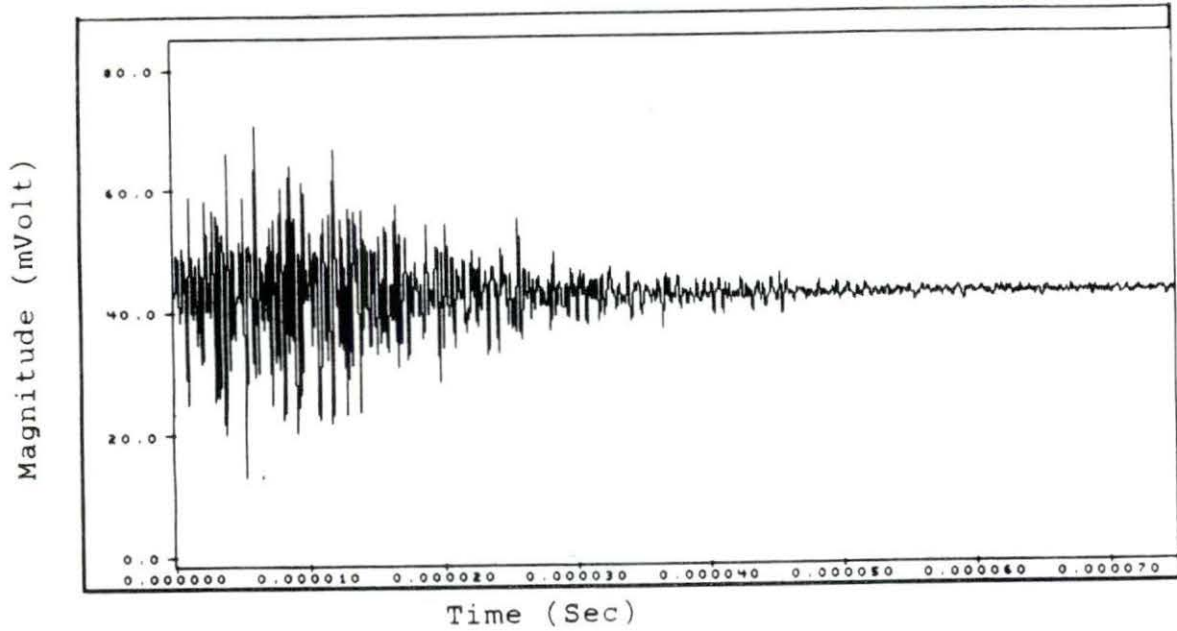
The Observation of the A-Mode Signal

Figure 4.10 shows the backscattered signals for one line of sight for a sample from each group (I-III) discussed above. These figures show that it is hard to tell the difference between them although all the pulser settings were kept the same (Gain=40 dB, Attenuation=4 dB, Damping=5). These results do not support the study done by Anselmo et al. (1987). Using the real-time signal (A-scan backscattered signal) as an objective read-out to show a good correlation with visual beef grading can be a misleading indicator. This result suggests

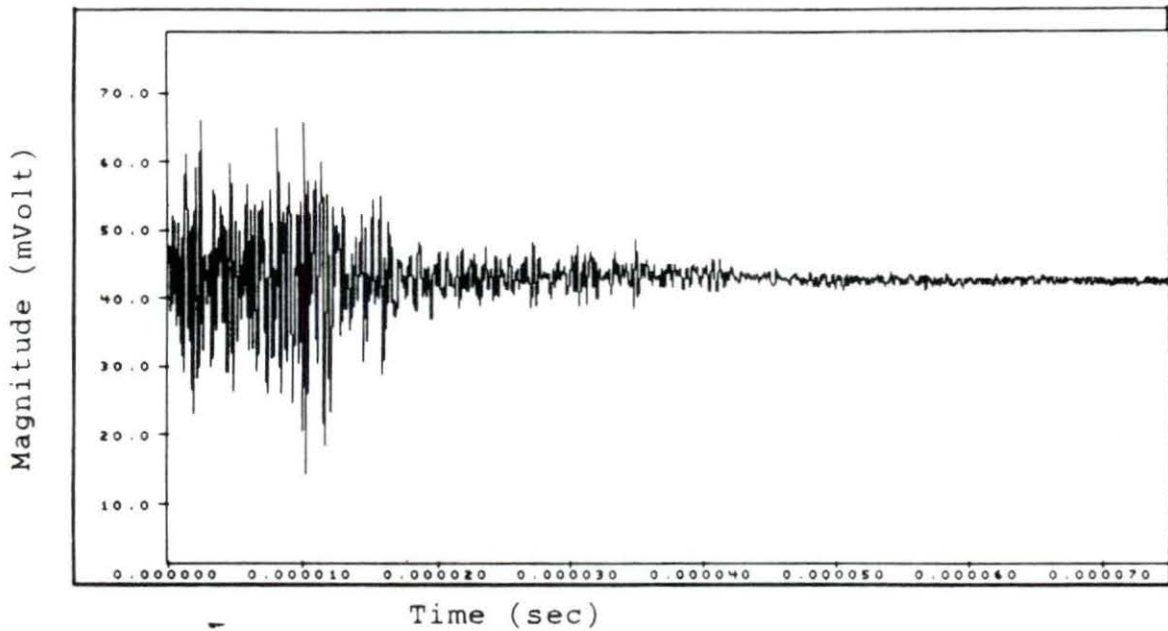
Table 4.6 The p-values for comparing the slopes of the attenuation coefficient of samples from the longissimus dorsi

H0: $\mu_{a1} = \mu_{a2}$	p-value
Prime - Choice(+)	0.0053
Prime - Choice	0.0001
Prime - Select(-)	0.0001
Choice(+)- Choice	0.0001
Choice(+)- Select(-)	0.0001
Choice - Select(-)	0.4359

that it is important to determine an indicator which is independent of the magnitude of the A-mode signal. The slope of the attenuation coefficient, measured using the least squares method, does not depend on the absolute magnitude of the signals. Instead, the slope of attenuation coefficient value depends on the relative magnitudes of the signals in the windowed segments.

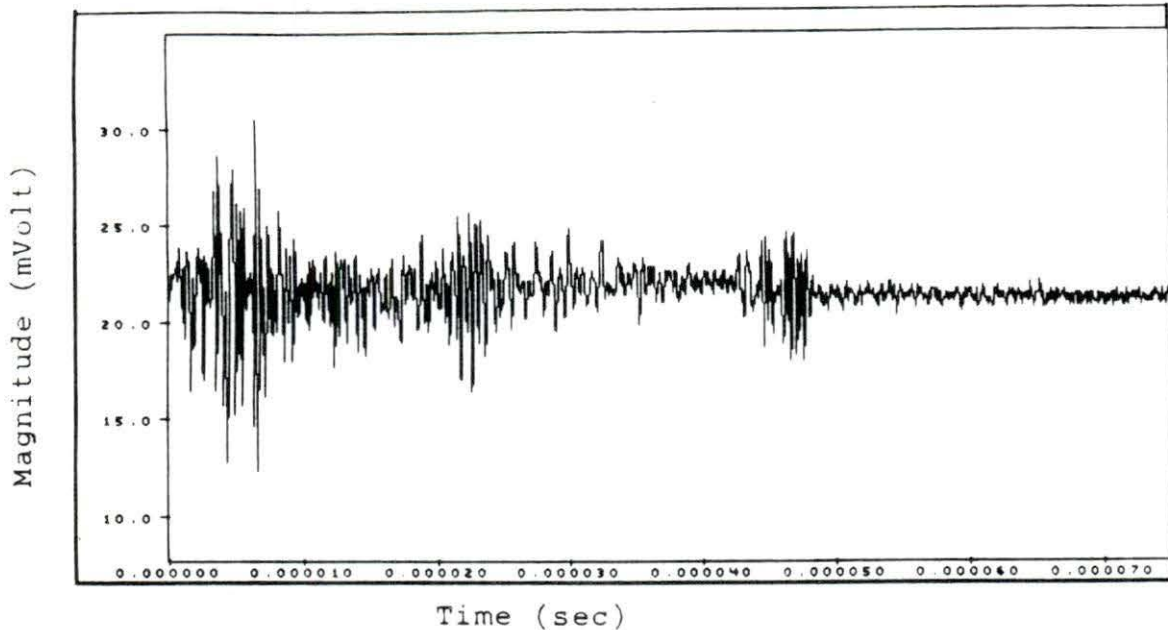


(a)



(b)

Figure 4.10 Backscattered signal from one line of sight of sample with fat percentage (a) 9.18 (b) 7.19



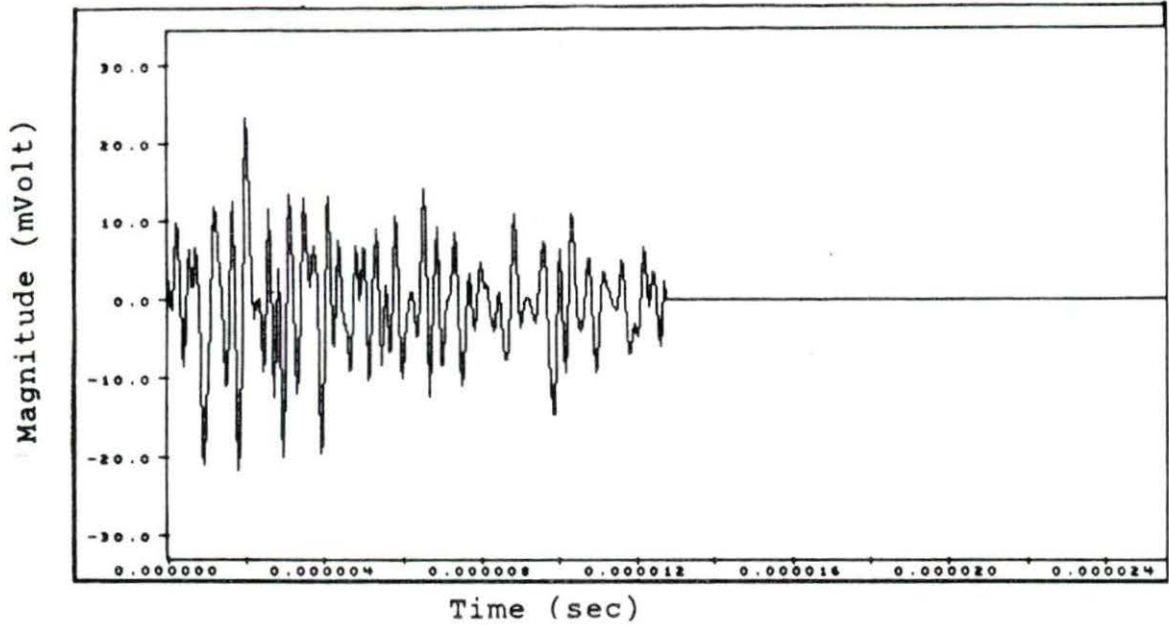
(c)

Figure 4.10 (continued) (c) 1.52

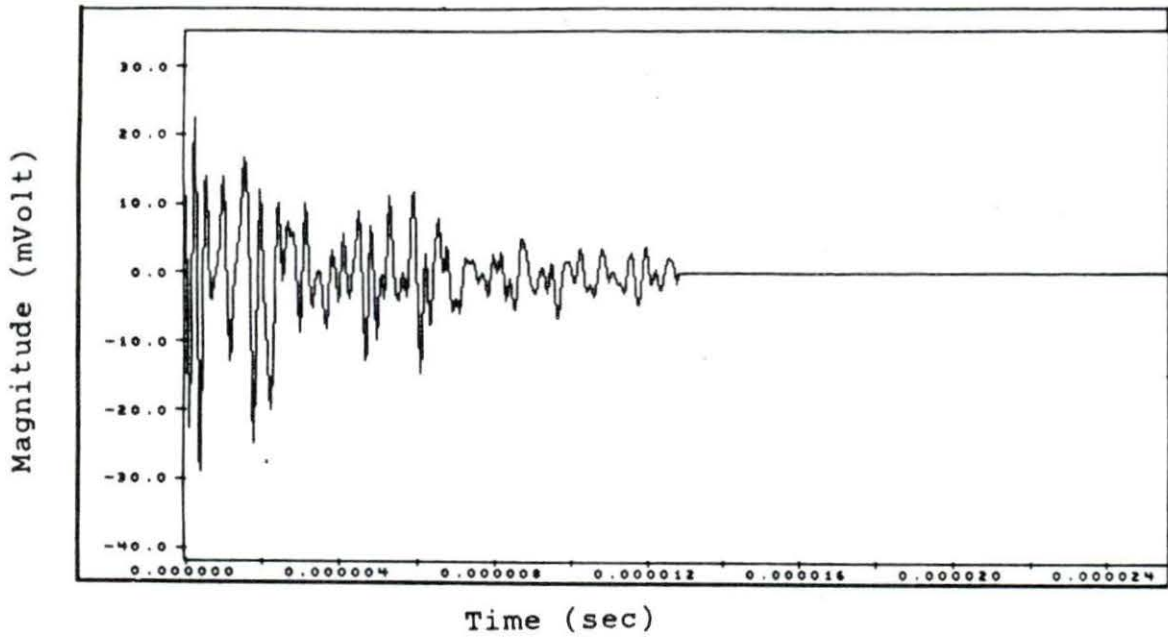
The Observation in the Power Spectra

Figure 4.11 displays the first window data signal of the samples that were taken to represent each group. Figure 4.12 (a), (b) and (c) illustrates the power spectra of the segmented signals in Figure 4.11. Figure 4.12 (a) and (b) shows more frequency response components than Figure 4.12 (c). By comparing these figures, it can be subjectively determined that the power spectra of Figure 4.12 (a) and (b) were taken from samples with more irregular borders and scatterers than the one which resulted in Figure 4.12 (c).

The results (Appendix A) also show that within the same bandwidth, the range of the frequency bandwidth shifted



(a)



(b)

Figure 4.11 The 1st segmentation data signal from a sample with percentage fat (a) 9.18 (b) 7.19

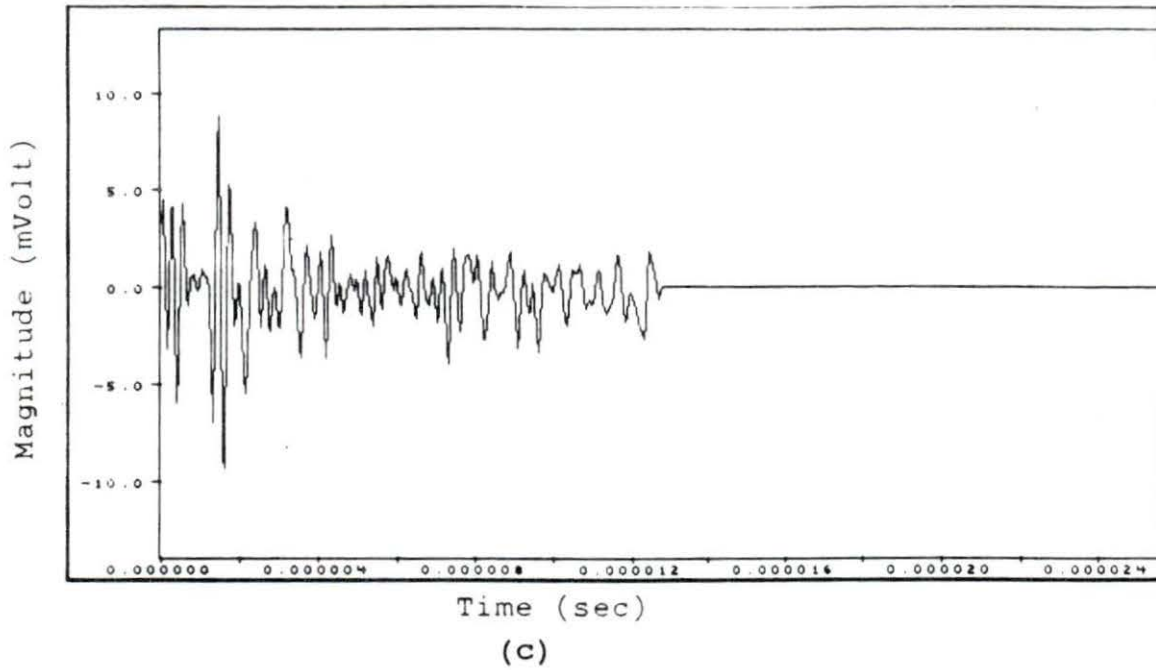


Figure 4.11 (continued) (c) 1.52

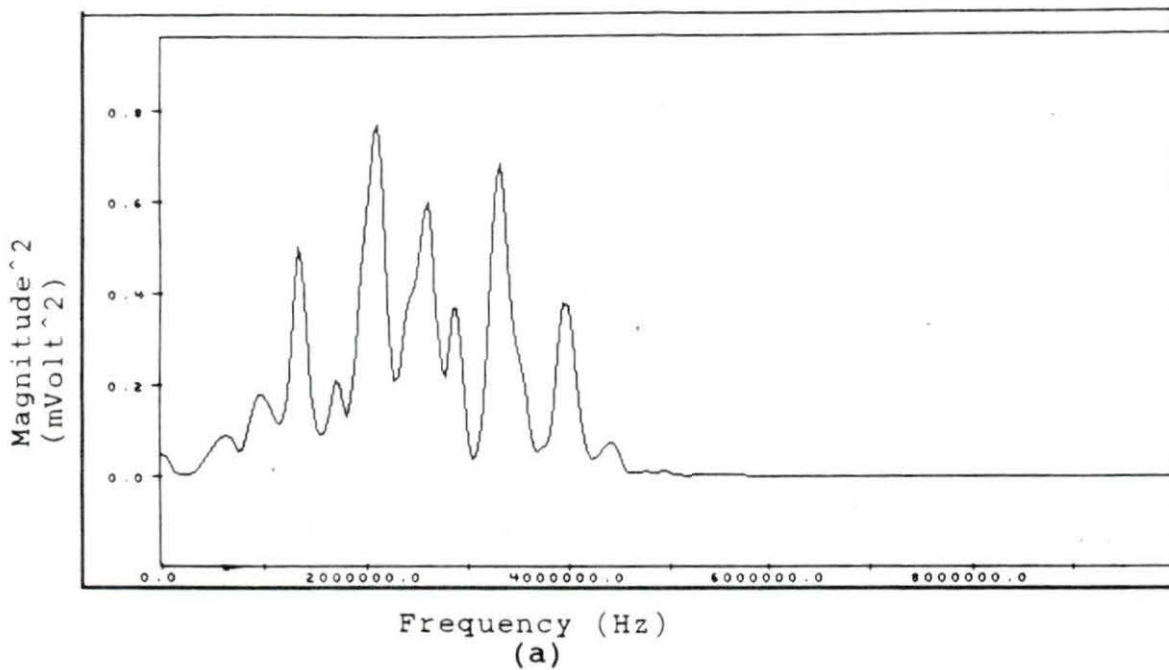
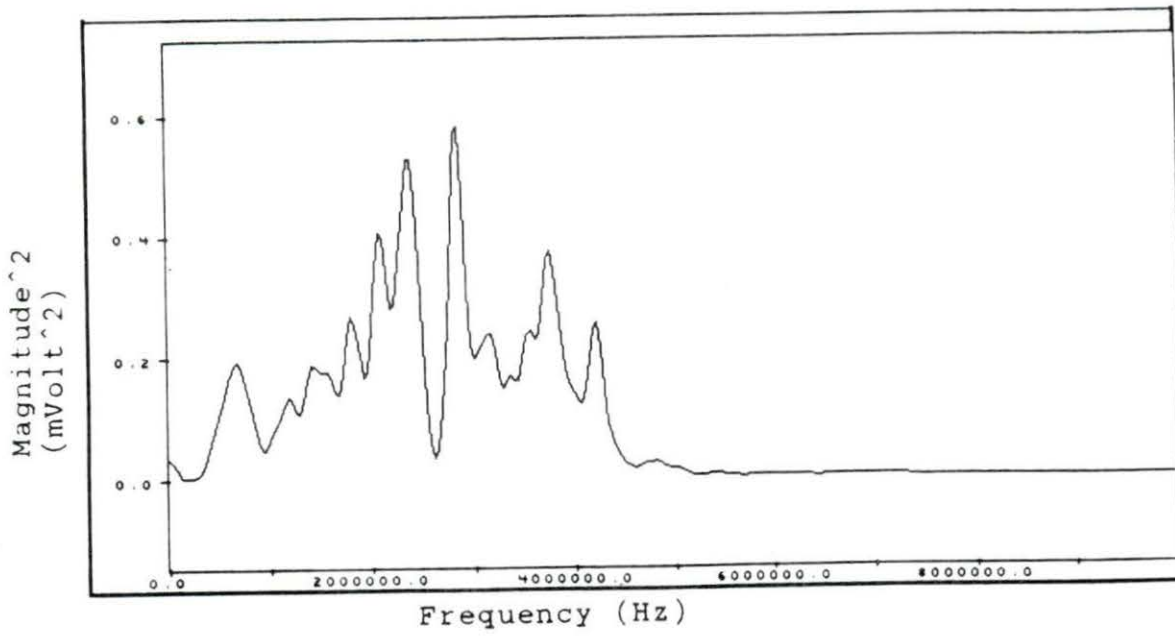
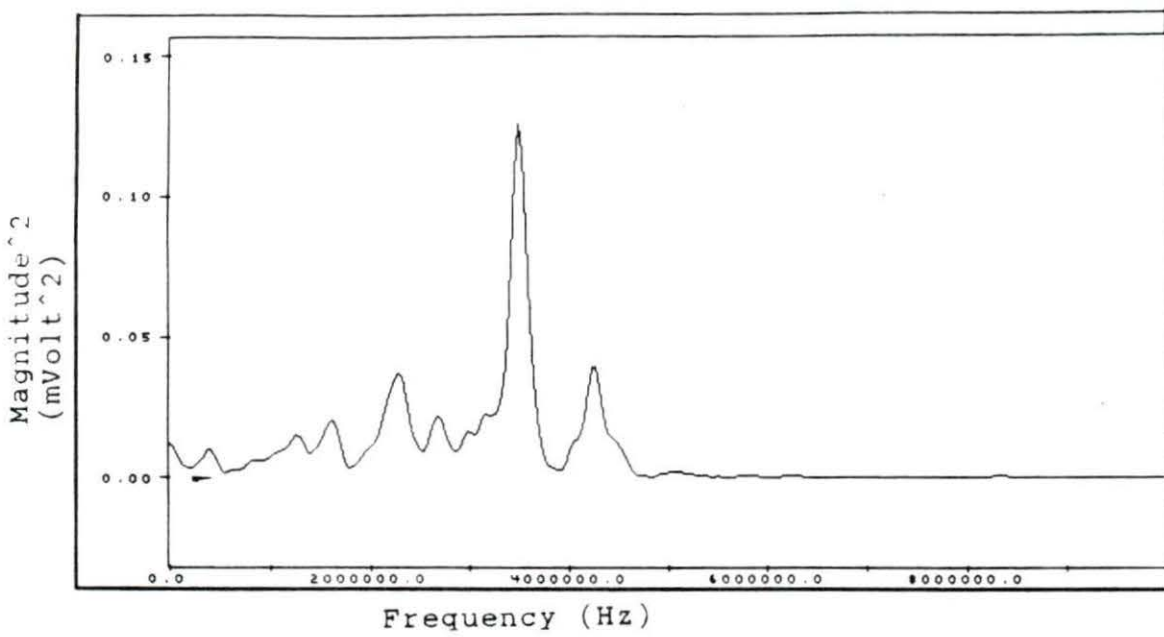


Figure 4.12 Frequency response of the 1st window from the sample with percentage fat (a) 9.18



(b)

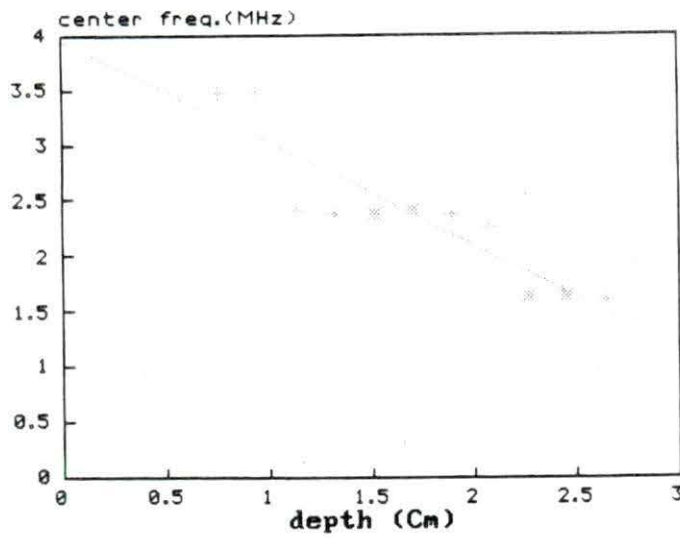


(c)

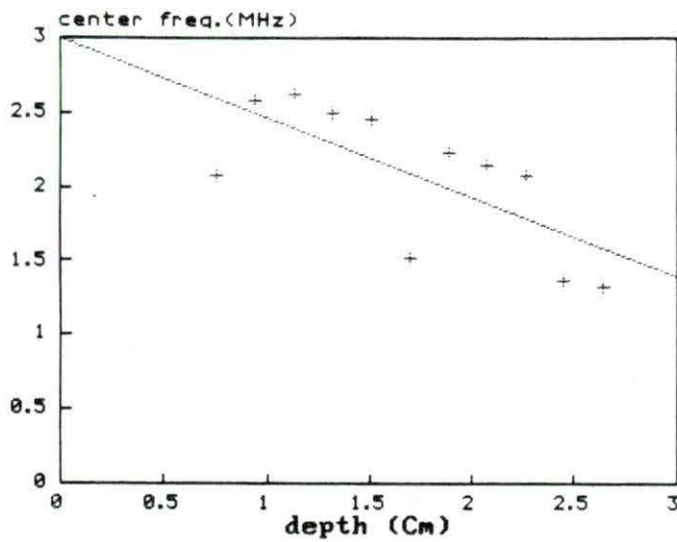
Figure 4.12 (continued) (b) 7.19 (c) 5.12

randomly in the low fat samples, group III, in which the slope of the attenuation coefficient ranged from 0.83 - 1.75 dB/cm-MHz. The range of the frequency bandwidth of the low fat samples varied randomly from 0.94 - 4.41 MHz to 1.91 - 5.39 MHz. However, the mean range of frequency bandwidth in the higher grades of fat samples was more consistent- between 1.52 - 5.00 MHz. The results agree with the results from previous experiments done by Chang (1991). His results showed more variation of the center frequency of lower fat percentage samples.

The center frequency (the maximum magnitude of the power spectrum) of each window segment within a line of sight was observed. One sample was taken from each group I, II, and III. It was concluded that the center frequency was downwardly shifted as the pulse went deeper into the sample. This conclusion is shown in Figure 4.13. Figure 4.13 demonstrates the linear regression of the center frequency at different depths in the samples. To test how significant the slope was, the data was run in the SAS program from the Wylber system. The hypothesis used was that there was no change in the center frequency data within 2.70 cm depth from each group. The programs and their results are submitted in the Appendix D. The results showed that the center frequency of the data from group I was shifted downward 0.4514 MHz as the transmitted pulse propagated one cm into the attenuating sample, with a p-

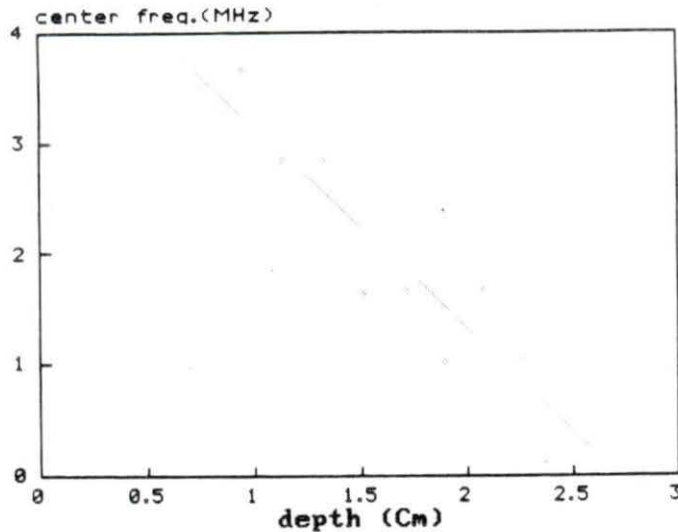


(a)



(b)

Figure 4.13 The correlation between the center frequency and the depth of the sample for a sample with percentage fat (a) 9.18 (b) 7.19



(c)

Figure 4.13 (continued) (c) 1.52

value of 0.0001. This means that the hypothesis above can be rejected with 0.01% error. The downward shifting of the center frequencies from groups II and III were 0.4491 MHz/cm and 0.7853 MHz/cm, respectively, with the p-values of 0.0006 and 0.0001.

Recommendation

These experiments suggest that the slope of the attenuation coefficient might be a good indicator to use to differentiate beef grades. The results suggest further study of the relationship of the attenuation coefficient and the frequency in different beef grades and finally using the slope

of the attenuation coefficient to differentiate the grades. The results of the attenuation studies in this experiment show a linear relationship between the slope of the attenuation coefficient and the percentage of fat. The attenuation of the prime group is distinctive; however, the ranges of slopes of the attenuation coefficient overlap in the lower grades. For further study, it is suggested that the number of the samples be increased to see if that will minimize the overlap between lower grade groups. It is assumed that the slopes of the attenuation coefficient for data samples are normally distributed, thus, with a greater number of data samples the approximation of the mean attenuation value becomes more precise.

From the frequency response from the sample in each group, it was observed that the bandwidth of the spectrum in the low grade sample varied more than the one in the high grade sample. It was also observed that the center frequency from the low grade samples shifted more with depth than that from the high grade samples. In further study, it is suggested that observation of the center frequency and bandwidth be emphasized to determine their usefulness in differentiating beef grades.

BIBLIOGRAPHY

- Amin, Viren R. 1989. Ultrasonic attenuation estimation for tissue characterization. Masters Thesis. Iowa State University.
- Anselmo, V.J., J. Clark and P.M. Gammell. 1987. Electronic inspection of beef. JPL invention Report NPO-15477/4352. (Jet Propulsion Laboratory, California Institute of Technology, Pasadena, California.)
- Boggs, Donald L. and Robert A. Merkel. 1979. Live Animal Carcass Evaluation and Selection Manual. Kendall/Hunt Publishing Company, Dubuque. 187pp.
- Chang, Alan. 1991. Utility of the backscattered ultrasonic A-mode signal for the quantitative grading of beef. Masters Thesis. Iowa State University.
- Christensen, D. A. 1988. Ultrasonic Bioinstrumentation. John Wiley & Sons, New York. 235 pp.
- Haumschild, D.J. and D.L. Carlson. 1983. An ultrasonic Bragg scattering technique for the quantitative characterization of marbling in beef. *Ultrasonics* 21:226-233.

- Javanaud, C. 1988. Applications of ultrasound to food systems. *Ultrasonics* 26:117-123.
- Kuc, Roman. 1980. Clinical application of an ultrasound attenuation coefficient estimation technique for liver pathology characterization. *IEEE Transactions on Biomedical Engineering* BME-27:312-319.
- Kuc, Roman and Mischa Schwartz. 1979. Estimating the acoustic attenuation coefficient slope for liver from reflected ultrasound signal. *IEEE Transactions on Sonic and Ultrasonics* SU-26:353-362.
- Kuc, Roman, Mischa Schwartz and Lajos Von Micsky. 1976. Parametric estimation of the acoustic attenuation coefficient slope for soft tissue. Pages 44-47 in 1976 *IEEE Ultrasonics Symposium Proceedings* (IEEE Cat.No.76 CH1120-5SU). IEEE, New York.
- Merkulova, V.M. 1967. Accuracy of the pulse method for measuring the attenuation and velocity of ultrasound. *Soviet Physics-Acoustics* 12, No 4:411-414.
- Narayana, Ponnada A. and Jonathan Ophir. 1983. On the frequency dependence of attenuation in normal and fatty liver. *IEEE Transactions on Sonics and Ultrasonics* SU-30:379-383.
- Proakis, John G. and Dimitris G. Manolakis. 1988. Introduction to Digital Signal Processing. Macmillan Publishing Company, New York. 944pp.

- Robinson, D.E. 1979. Computer spectral analysis of ultrasonic A-mode echoes. Pages 281-286 in M.Linzer, ed. Ultrasonic Tissue Characterization II. National Bureau of Standards Special Publication 525. U.S. Government Printing Office, Washington, D.C.
- Round, W.H. and Bates, R.H.T. 1987. Modification of spectra of pulses from ultrasonic transducers by scatterers in non-attenuating and in attenuating media. *Ultrasonic Imaging* 9:18-28.
- Savell, J.W., R.H. Cross and G.C. Smith. 1986. Percentage ether extractable fat and moisture content of beef longissimus muscle as related to USDA marbling score. *J Food Science* 51(3):838-840.
- Shung, k. Kirk. 1987. General engineering principles in diagnostic ultrasound. *IEEE Engineering in Medicine and Biology Magazine* 6:7-13.
- Wilson, L.S., D.E. Robinson and B.D. Doust. 1984. Frequency domain processing for ultrasonic attenuation measurement in liver. *Ultrasonic Imaging* 6:278-292.

ACKNOWLEDGEMENTS

I would like to thank my major professor, Dr David L. Carlson, for giving me the opportunity to work with him in this research. I am thankful for his support to make this work possible. I also would like to express my gratitude to Dr Mary Helen Greer, Dr Curran Swift, and Dr Richard Horton for their time and thoughtful suggestions in helping and encouraging me to write this thesis.

I am also thankful to Anila Lingamneni, Mike Hofstad, Curtis Olson, Kyle Holland, Alan Chang, Viren Amin, Vincent Doerr and other friends in BME and MUDIKA for sharing their friendships, knowledge, interests, and humors during my stay in Ames. I really love their company. Being friends with them has been very enjoyable and an unforgettable experiences to me.

My deep appreciation also goes to very special people in my life: my parents, my grandparents, my brother, Sugiharto Ongkowijoyo, and Edith Gozali, for their love, support, and understanding so that I can do my best.

APPENDIX A
RESULTS OF EXPERIMENTS

Table A1

Sampling Rate : 20 MHz Pulser Settings : page 22 % Fat : 10.88 Location : Lateral end				
Angle	1st Window depth (cm)	Number of windows	Bandwidth (MHz)	a dB/cm-MHz
0	0.7623	11	1.52-5.00	2.27
2.5	0.7623	11	1.52-5.00	1.51
5	0.9510	11	1.52-5.00	2.85
7.5	0.9510	11	1.52-5.00	2.41
10	0.9510	11	1.56-5.04	3.03
- 2.5	0.7623	11	1.52-5.00	1.90
- 5	0.5737	10	1.52-5.00	2.36
- 7.5	0.7623	11	1.52-5.00	2.03
-10	0.9510	11	1.52-5.00	2.35

Table A2

Sampling Rate : 20 MHz Pulser Settings : page 22 % Fat : 9.18 Location : Medial end				
Angle	1st Window depth (cm)	Number of windows	Bandwidth (MHz)	a dB/cm-MHz
0	0.7623	11	1.52-5.00	2.86
2.5	0.5737	9	1.56-5.04	2.40
5	0.3850	12	1.56-5.04	2.17
7.5	0.3850	12	1.56-5.04	2.17
10	0.5737	12	1.37-4.84	1.51
- 2.5	0.5737	12	1.56-5.04	1.62
- 5	0.7623	11	1.56-5.04	3.30
- 7.5	0.7623	11	1.56-5.04	1.89
-10	0.5737	11	1.56-5.04	2.47

Table A3

Sampling Rate : 20 MHz Pulser Settings : page 22 % Fat : 5.20 Location : Lateral end at proximal border				
Angle	1st window depth (cm)	Number of windows	Bandwidth (MHz)	a dB/cm-MHz
0	0.3850	8	1.52 -5.00	2.67
2.5	0.5737	11	1.56 -5.04	1.63
5	0.5737	11	1.56 -5.04	1.42
7.5	0.5737	10	1.56 -5.04	2.75
10	0.5737	9	1.76 -5.24	1.96
- 2.5	0.5737	10	1.56 -5.04	1.62
- 5	0.5737	9	1.56 -5.04	1.62

Table A4

Sampling Rate : 20 MHz Pulser Settings : page 22 % Fat : 7.19 Location : Lateral end below acorn fat depot				
Angle	1st window depth (cm)	Number of windows	Bandwidth (MHz)	a dB/cm-MHz
0	0.7623	9	1.52 -5.00	1.71
2.5	0.7623	11	1.37 -4.84	1.16
5	0.7623	9	1.52 -5.00	1.86
7.5	0.9510	11	1.52 -5.00	1.91
10	0.9510	11	1.52 -5.00	1.71
- 2.5	0.5737	10	1.52 -5.00	2.03
- 5	0.5737	9	1.52 -5.00	1.86
- 7.5	0.3850	9	1.41 -4.88	1.88
-10	0.7623	11	1.52 -5.00	1.66

Table A5

Sampling Rate : 20 MHz Pulser Settings : page 22 % Fat : 9.45 Location : Medial end below acorn fat depot				
Angle	1st window depth (cm)	Number of windows	Bandwidth (MHz)	a dB/cm-MHz
0	0.5737	12	1.56 -5.04	2.15
2.5	0.7623	12	1.56 -5.04	2.21
5	0.7623	12	1.33 -4.80	1.29
7.5	0.7623	12	1.52 -5.00	1.71
10	0.7623	12	1.37 -4.84	2.39
- 2.5	0.3850	14	1.37 -4.84	1.87
- 5	0.5737	11	1.52 -5.00	1.95
- 7.5	0.5737	11	1.68 -5.16	2.63
-10	0.5737	11	1.52 -5.00	1.66

Table A6

Sampling Rate : 20 MHz Pulser Settings : page 22 % Fat : 8.85 Location : Medial end at distal border				
Angle	1st window depth (cm)	Number of windows	Bandwidth (MHz)	a dB/cm-MHz
0	1.3283	10	1.52 -5.00	1.88
2.5	0.9510	11	1.52 -5.00	2.94
5	0.9510	10	1.37 -4.84	1.68
7.5	0.9510	10	1.68 -5.16	2.18
10	0.7623	10	1.52 -5.00	1.98
- 2.5	0.7623	10	1.52 -5.00	2.46
- 5	0.5737	10	1.52 -5.00	1.70
- 7.5	0.9510	10	1.52 -5.00	1.45
-10	0.7623	9	1.37 -4.84	1.57

Table A7

Sampling Rate : 20 MHz Pulser Settings : page 22 % Fat : 3.56 Location : Lateral end				
Angle	1st window depth (cm)	Number of windows	Bandwidth (MHz)	a dB/cm-MHz
0	0.3850	9	1.84 -5.31	1.16
5	0.5737	9	1.25 -4.73	1.16
7.5	0.5737	9	0.94 -4.41	1.18
10	0.5737	9	1.25 -4.73	1.83
- 2.5	0.3850	9	1.52 -5.00	1.74
- 7.5	0.3850	10	1.52 -5.00	1.11
-10	0.3850	11	1.68 -5.16	1.55

Table A8

Sampling Rate : 20 MHz Pulser Settings : page 22 % Fat : 1.52 Location : medial end				
Angle	1st window depth (cm)	number of windows	Bandwidth (MHz)	a dB/cm-MHz
0	0.3850	11	1.91 -5.39	0.99
2.5	0.5737	11	1.91 -5.39	0.33
5	0.7623	12	1.91 -5.39	1.11
7.5	0.5737	12	1.91 -5.39	1.18
10	0.5737	11	1.91 -5.39	1.10
- 2.5	0.5737	10	1.37 -4.84	0.51
- 5	0.7623	9	1.37 -4.84	1.30
- 7.5	0.9510	9	1.37 -4.84	0.36
-10	0.9510	9	1.37 -4.84	0.59

Table A9

Sampling Rate : 20 MHz Pulser Settings : page 22 % Fat : 2.74 Location : Lateral end at distal border				
Angle	1st window depth (cm)	Number of windows	Bandwidth (MHz)	a dB/cm-MHz
0	0.3850	9	1.52 -5.00	1.82
2.5	0.3850	9	1.52 -5.00	0.57
5	0.5737	9	1.25 -4.73	0.85
7.5	0.3850	10	1.52 -5.00	1.20
10	0.3850	9	1.76 -5.24	1.75
- 2.5	0.5737	9	1.52 -5.00	1.79
- 5	0.3850	11	1.68 -5.16	1.64
- 7.5	0.5737	9	1.52 -5.00	1.26
-10	0.5737	11	1.68 -5.16	1.01

Table A10

Sampling Rate : 20 MHz Pulser Settings : page 22 % Fat : 2.28 Location : Medial end below acorn fat depot				
Angle	1st window depth (cm)	Number of windows	Bandwidth (MHz)	a dB/cm-MHz
0	0.7623	9	1.52 -5.00	0.82
2.5	0.7623	11	1.52 -5.00	0.80
7.5	0.3850	11	1.52 -5.00	1.37
10	0.3850	11	1.52 -5.00	1.97
- 2.5	0.5737	9	1.25 -4.73	1.17
- 5	0.5737	11	1.45 -4.92	0.86
- 7.5	0.5737	9	1.37 -4.84	1.12
-10	0.5737	11	1.52 -5.00	0.99

APPENDIX B

MOISTURE/FAT DETERMINATION (CHANG, 1991)

Ether extraction method**Theory**

The sample is weighed, dried, cooled, and then reweighed. The weight loss is calculated as moisture content. The sample is then used for the fat extractor, and fat is removed using the petroleum ether. The sample is extracted, dried and reweighed to determined fat content.

Equipment and chemicals

Whatman 22 X 80 cellulose extraction thimbles (dried at least 2 hours and stored in desiccator)

Weighing spatulas

Balance

Drying oven

Petroleum ether

Cotton

Desiccator

Procedure

- 1) Weight dried thimble, record weight (A), and tare the balance. The thimbles collect moisture, so work rapidly and do not touch them with your hands. If the samples are >20% fat, dried cotton should be put in the bottom of the thimble and included in the thimble weight. This is done to absorb any fat that could leak out during the initial drying of the sample.
- 2) Using a spatula, transfer 5g of ground, emulsified, or blended sample into the tared thimble and record the weight (B).
- 3) Place sample in drying oven for at least 18 hours.
- 4) Remove sample from oven and allow to cool in a desiccator and weigh to get the dried weight (C).
- 5) Run the dried sample to the Soxhlet fat extractor for at least 6 hours.
- 6) After extraction, samples should be dried in the drying oven for at least 2 hours.
- 7) Remove samples from the oven and allow to cool in a desiccator and weigh to get the extracted weight (D). The sample can then be discarded.

Calculations

$$\% \text{ Moisture} = 100 [B - (C-A)] / B$$

$$\% \text{ Fat} = 100 [(C-A) - (D-A)] / B$$

APPENDIX C

SIGNAL PROCESSING PROGRAM

```

*****
'* PURPOSE : to compute the power spectrum of each *
'*           window segment                          *
'* written by : Lanny B Widyaatmadja                *
*****

DECLARE SUB FILTER (XR!(), PHI!)
DECLARE SUB PHASE (WR!(), WI!(), N%, PHI!)
DECLARE SUB FFT (XR!(), XI!(), WR!(), WI!(), N%, PD!(), Z%)

DIM SHARED D(1500) AS SINGLE
DIM SHARED XR(512) AS SINGLE
DIM SHARED XI(512) AS SINGLE
DIM SHARED WR(512) AS SINGLE
DIM SHARED WI(512) AS SINGLE
DIM SHARED PD(512) AS SINGLE

'* Devide the input signal into 512 window segment

INPUT "how many window ?", W%
A1$ = "B:\BF6\NDT\"
INPUT "input filename :", A2$
A$ = A1$ + A2$
OPEN "I", #1, A$
FOR I% = 1 TO 1500
    INPUT #1, D!(I%)
NEXT I%
C$ = "B:\DEPTH.1"
OPEN C$ FOR APPEND AS #3
PHI! = 3.14159
INPUT "starting pnt of window:", S%
FOR J% = 1 TO W%
    DC! = 127
    PRINT "DC voltage:", DC!
    PRINT "starting pnt of window:", S%
    START% = S%
    FOR L% = 1 TO 256
        XR!(L%) = (D!(S%) - DC!) * (5 / 30)
        S% = S% + 1
    NEXT L%
    FOR K% = 257 TO 512
        XR!(K%) = 0
    NEXT K%
'* compute the autocorrelation for smoothing

    PRINT "calling FILTER subroutine"
    PHI! = 3.14159
    CALL FILTER(XR!(), PHI!)
    N% = 512
'* compute the power spectra

    PRINT "calling PHASE subroutine"
    CALL PHASE(WR!(), WI!(), N%, PHI!)
    PRINT "calling FFT subroutine "
    Z% = J%
    CALL FFT(XR!(), XI!(), WR!(), WI!(), N%, PD!(), Z%)
    DEPTH! = (START% * (1 / 2E+07) * 154000) / 2
    WNW% = Z%
    PRINT "window:", WNW%
    WRITE #3, WNW%, DEPTH!
    S% = START% + 49
NEXT J%
CLOSE #1
CLOSE #3
END

```



```

SUB FFT (XR!(), XI!(), WR!(), WI!(), N%, PD!(), Z%)

FOR I% = 1 TO 15
  M% = I%
  N2% = 2 ^ I%
  IF (N% = N2%) GOTO FFT
NEXT I%
PRINT "N is not a power of two"
STOP

FFT:

FOR G% = 1 TO 512
  XI!(G%) = 0
NEXT G%
N2% = N%
FOR I% = 1 TO M%
  N1% = N2%
  N2% = N2% / 2
  I1% = 1
  I2% = N% / N1%
  FOR J% = 1 TO N2%
    C! = WR!(I1%)
    S! = WI!(I1%)
    I1% = I1% + I2%
    FOR K% = J% TO N% STEP N1%
      L% = K% + N2%
      TEMPR! = XR!(K%) - XR!(L%)
      XR!(K%) = XR!(K%) + XR!(L%)
      TEMPI! = XI!(K%) - XI!(L%)
      XI!(K%) = XI!(K%) + XI!(L%)
      XR!(L%) = C! * TEMPR! + S! * TEMPI!
      XI!(L%) = C! * TEMPI! - S! * TEMPR!
    NEXT K%
  NEXT J%
NEXT I%

BITREV:
J% = 1
N1% = N% - 1
FOR I% = 1 TO N1%
  IF (I% >= J%) GOTO A
  TEMP! = XR!(J%)
  XR!(J%) = XR!(I%)
  XR!(I%) = TEMP!
  TEMP! = XI!(J%)
  XI!(J%) = XI!(I%)
  XI!(I%) = TEMP!
A:
B:
  K% = N% / 2
  IF (K% >= J%) GOTO C
  J% = J% - K%
  K% = K% / 2
  C:

```

```

      GOTO B
C:      J% = J% + K%
NEXT I%
E1$ = "B:\PWR."
E$ = E1$ + STR$(-Z%)
PRINT "power spectrum density filename=", E$
OPEN "0", #7, E$
FOR J% = 1 TO N%
    PD!(J%) = (XR!(J%) ^ 2 + XI!(J%) ^ 2) / N%
    WRITE #7, PD!(J%)
NEXT J%
CLOSE #7

END SUB

SUB FILTER (XR!( ), PHI!)

DIM AUTO!(0 TO 511), HAMM!(128 TO 256), AXR!(0 TO 511)

FOR L% = 0 TO 511
    AUTO!(L%) = XR!(L% + 1)
NEXT L%
FOR L% = 0 TO 511
    SUM! = 0
    FOR G% = 0 TO 511 - L%
        SUM! = SUM! + (AUTO!(G%) * AUTO!(G% + L%))
    NEXT G%
    AXR!(L%) = (1 / 512) * SUM!
NEXT L%
PHI! = 3.14159

FOR K% = 128 TO 256
    HAMM!(K%) = .54 - .46 * COS((2 * PHI! * K%) / 256)
NEXT K%
PRINT "calculating autocor"
FOR J% = 1 TO 128
    XR!(J%) = 0
NEXT J%
DECR% = 256
XDECR% = 128
FOR K% = 129 TO 256
    XR!(K%) = AXR!(XDECR%) * HAMM!(DECR%)
    DECR% = DECR% - 1
    XDECR% = XDECR% - 1
NEXT K%
INCR% = 0
FOR L% = 257 TO 384
    XR!(L%) = AXR!(INCR%) * HAMM!(128 + INCR%)
    INCR% = INCR% + 1
NEXT L%
FOR M% = 385 TO 512
    XR!(M%) = 0
NEXT M%

END SUB

SUB PHASE (WR!( ), WI!( ), N%, PHI!)

FOR I% = 1 TO N%
    P! = (2 * PHI! * (I% - 1)) / N%
    WR!(I%) = COS(P!)
    WI!(I%) = SIN(P!)
NEXT I%

END SUB

```

```
'*****
'* Purpose : To compute the attenuation slope *
'*          using the least square method *
'* Written by : Lanny B Widyaatmadja *
'******
```

```
DECLARE SUB LOGA (D!(), X!(), I%)
DECLARE SUB slope (T!(), DEP!(), BETA!, W%)
DECLARE SUB REG (B!(), freq!(), BAND%, ATTN!)
```

```
DIM SHARED B(89) AS SINGLE
DIM SHARED freq(89) AS SINGLE
DIM SHARED T(11) AS SINGLE
DIM SHARED DEP(11) AS SINGLE
DIM SHARED X(40 TO 129) AS SINGLE
DIM SHARED D(512) AS SINGLE
DIM Z!(985)
```

```
'* Reading the data file from windows
```

```
INPUT "how many windows ?", W%
R$ = "B:\BAND.1"
OPEN R$ FOR APPEND AS #2
INCR% = 0
FOR I% = 1 TO W%
  A1$ = "B:\PWR."
  A$ = A1$ + STR$(-I%)
  OPEN "I", #1, A$
  FOR J% = 1 TO 512
    INPUT #1, D!(J%)
  NEXT J%
```

```
'* Compute the log spectra within bandwidth
```

```
PRINT "calling LOGARITHM subroutine"
CALL LOGA(D!(), X!(), I%)
ADD% = 1
FOR K% = 40 TO 129
  Z!((INCR% * 89) + ADD%) = X!(K%)
  WRITE #2, Z!((INCR% * 89) + ADD%)
  ADD% = ADD% + 1
NEXT K%
INCR% = INCR% + 1
CLOSE #1
NEXT I%
INPUT "# of freq. in bandwidth:", BAND%
K% = 1
G$ = "B:\DEPTH.2"
OPEN "I", #5, G$
FOR M% = 1 TO W%
  INPUT #5, DEP!(M%)
NEXT M%
H$ = "B:\FRQCY.1"
OPEN "I", #4, H$
FOR V% = 1 TO 89
  INPUT #4, freq(V%)
NEXT V%
J$ = "B:\SLOFREQ.1"
OPEN "O", #3, J$
FOR L% = 1 TO BAND%
  FOR Y% = 1 TO W%
    U% = K% + (89 * (Y% - 1))
    T!(Y%) = Z!(U%)
  NEXT Y%
```

```

* calculating slope of mag vs depth at particular freq
CALL slope(T!(), DEP!(), BETA!, W%)
PRINT "attn. slope:", BETA!
K% = K% + 1
B!(L%) = BETA!
WRITE #3, BETA!, freq!(L%)
NEXT L%
* calculating attn. slope (attn vs freq)
CALL REG(B!(), freq!(), BAND%, ATTNS!)
PRINT "attn. slope (db/Cm.Mhz):", ATTNS!
CLOSE #2
CLOSE #3
CLOSE #4
CLOSE #5
END

SUB LOGA (D!(), X!(), I%)

DIM LD!(256)
MAX! = D!(1)
FOR L% = 1 TO 256
  IF (MAX! <= D!(L%)) THEN
    MAX! = D!(L%)
  END IF
NEXT L%
FOR K% = 1 TO 256
  LD!(K%) = 10 * (LOG(D!(K%)) / LOG(10!))
  IF (K% >= 40) AND (K% <= 129) THEN
    X!(K%) = LD!(K%)
  END IF
NEXT K%

END SUB

SUB REG (B!(), freq!(), BAND%, ATTNS!)
SUMF! = 0!
SUMA! = 0!
SUMFF! = 0!
SUMFA! = 0!

FOR Y% = 1 TO BAND%
  SUMF! = SUMF! + (freq!(Y%) * .000001)
  SUMA! = SUMA! + B!(Y%)
  FA! = (freq!(Y%) * .000001) * B!(Y%)
  FF! = (freq!(Y%) * .000001) * (freq!(Y%) * .000001)
  SUMFF! = SUMFF! + FF!
  SUMFA! = SUMFA! + FA!
NEXT Y%
SQRF! = SUMF! * SUMF!
ATTNS! = (SUMFA! - ((SUMF! * SUMA!) / BAND%)) / (SUMFF! - (SQRF! / BAND%))
PRINT "SUM OF X=", SUMF!
PRINT "SUM OF Y=", SUMA!
PRINT "(SUM OF X)^2=", SQRF!
PRINT "SUM OF (X*Y)=", SUMFA!
PRINT "SUM OF (Y^2)=", SUMFF!

END SUB

SUB slope (T!(), DEP!(), BETA!, W%)

SUMX! = 0!
SUMY! = 0!
SUMXX! = 0!
SUMXY! = 0!

```

```
FOR I% = 1 TO W%
  SUMX! = SUMX! + DEP!(I%)
  SUMY! = SUMY! + T!(I%)
  XY! = DEP!(I%) * T!(I%)
  XX! = DEP!(I%) * DEP!(I%)
  SUMXX! = SUMXX! + XX!
  SUMXY! = SUMXY! + XY!
NEXT I%
SQRXX! = SUMX! * SUMX!
BETA! = (SUMXY! - ((SUMX! * SUMY!) / W%)) / (SUMXX! - (SQRXX! / W%))

END SUB
```

APPENDIX D
STATISTICAL ANALYSIS

Purpose : to group the sample data by testing the slope of the
attenuation coefficient mean value of each sample

```
1. // JOB
2. // EXEC SAS
3. OPTIONS LS=65;
4. DATA A; INPUT FAT ATTN; CARDS;
5. 10.88 2.35
6. 10.88 2.03
7. 10.88 2.36
8. 10.88 1.90
9. 10.88 2.27
10. 10.88 1.51
11. 10.88 2.85
12. 10.88 2.41
13. 10.88 3.03
14. 9.45 1.66
15. 9.45 2.63
16. 9.45 1.95
17. 9.45 1.87
18. 9.45 2.15
19. 9.45 2.21
20. 9.45 1.29
21. 9.45 1.71
22. 9.45 2.39
23. 9.18 2.47
24. 9.18 1.89
25. 9.18 3.30
26. 9.18 1.62
27. 9.18 2.86
28. 9.18 2.40
29. 9.18 2.17
30. 9.18 2.17
31. 9.18 1.51
32. 8.85 1.57
33. 8.85 1.45
34. 8.85 1.70
35. 8.85 2.46
36. 8.85 1.88
37. 8.85 2.94
38. 8.85 1.68
39. 8.85 2.18
40. 8.85 1.98
41. 7.19 1.66
42. 7.19 1.88
43. 7.19 1.86
44. 7.19 2.03
45. 7.19 1.71
```

46.	7.19	1.16
47.	7.19	1.86
48.	7.19	1.91
49.	7.19	1.71
50.	5.20	1.62
51.	5.20	1.62
52.	5.20	2.67
53.	5.20	1.63
54.	5.20	1.42
55.	5.20	2.75
56.	5.20	1.96
57.	3.56	1.55
58.	3.56	1.11
59.	3.56	1.74
60.	3.56	1.16
61.	3.56	1.16
62.	3.56	1.18
63.	3.56	1.83
64.	2.74	1.01
65.	2.74	1.26
66.	2.74	1.64
67.	2.74	1.79
68.	2.74	1.82
69.	2.74	0.57
70.	2.74	0.85
71.	2.74	1.20
72.	2.74	1.75
73.	2.28	0.99
74.	2.28	1.12
75.	2.28	0.86
76.	2.28	1.17
77.	2.28	0.82
78.	2.28	0.80
79.	2.28	1.37
80.	2.28	1.97
81.	1.52	0.59
82.	1.52	0.36
83.	1.52	1.30
84.	1.52	0.51
85.	1.52	0.99
86.	1.52	0.33
87.	1.52	1.11
88.	1.52	1.18
89.	1.52	1.10
90.	PROC GLM; CLASS FAT; MODEL ATTN=FAT; MEANS FAT;	
91.	CONTRAST '10 VS 9' FAT 0 0 0 0 0 0 0 0 -1 1;	
92.	CONTRAST '10 VS 8' FAT 0 0 0 0 0 0 0 0 -1 0 1;	
93.	CONTRAST '10 VS 7' FAT 0 0 0 0 0 0 0 -1 0 0 1;	
94.	CONTRAST '10 VS 6' FAT 0 0 0 0 0 0 -1 0 0 0 1;	
95.	CONTRAST '10 VS 1' FAT -1 0 0 0 0 0 0 0 0 0 1;	
96.	CONTRAST '10 VS 4' FAT 0 0 0 -1 0 0 0 0 0 0 1;	
97.	CONTRAST '10 VS 3' FAT 0 0 -1 0 0 0 0 0 0 0 1;	
98.	CONTRAST '10 VS 2' FAT 0 -1 0 0 0 0 0 0 0 0 1;	
99.	CONTRAST '10 VS 5' FAT 0 0 0 0 -1 0 0 0 0 0 1;	
100.	CONTRAST '10,9,8,7,6 VS 1,2,3,4,5' FAT -5 -5 -5 -5 5 5 5 5 5 5;	
101.	CONTRAST '10,8 VS 1,6,7,9' FAT -2 0 0 0 0 -2 -2 4 -2 4;	
102.	CONTRAST '10,8 VS 3,4' FAT 0 0 -2 -2 0 0 0 2 0 2;	
103.	CONTRAST '10,8 VS 2,5' FAT 0 -2 0 0 -2 0 0 2 0 2;	
104.	CONTRAST '1,6,7,9 VS 3,4' FAT 2 0 -4 -4 0 2 2 0 2 0;	
105.	CONTRAST '1,6,7,9 VS 2,5' FAT 2 -4 0 0 -4 2 2 0 2 0;	
106.	CONTRAST '2,5 VS 3,4' FAT 0 2 -2 -2 2 0 0 0 0 0;	

General Linear Models Procedure
Class Level Information

Class	Levels	Values
FAT	10	5.2 1.52 2.28 2.74 3.56 7.19 8.85 9.18 9.45 10.88

Number of observations in data set = 85

The SAS System 2
21:28 Monday, September 16, 1991

General Linear Models Procedure

Dependent Variable: ATTN

Source	DF	Sum of Squares	F Value	Pr > F
Model	9	19.35688701	11.36	0.0001
Error	75	14.20047063		
Corrected Total	84	33.55735765		

R-Square	C.V.	ATTN Mean
0.576830	25.60662	1.69929412

Source	DF	Type I SS	F Value	Pr > F
FAT	9	19.35688701	11.36	0.0001

Source	DF	Type III SS	F Value	Pr > F
FAT	9	19.35688701	11.36	0.0001

The SAS System 3
21:28 Monday, September 16, 1991

General Linear Models Procedure

Level of	-----ATTN-----		
FAT	N	Mean	SD
5.2	7	1.95285714	0.54153222
1.52	9	0.83000000	0.37934153
2.28	8	1.13750000	0.38949601
2.74	9	1.32111111	0.45492979
3.56	7	1.39000000	0.30822070
7.19	9	1.75333333	0.25109759
8.85	9	1.98222222	0.47688515
9.18	9	2.26555556	0.57339147
9.45	9	1.98444444	0.40875149

10.88 9 2.30111111 0.46253228
 The SAS System
 21:28 Monday, September 16, 1991

General Linear Models Procedure

Dependent Variable: ATTN

Contrast	DF	Contrast SS	F Value	Pr > F
10 VS 9	1	0.45125000	2.38	0.1268
10 VS 8	1	0.00568889	0.03	0.8629
10 VS 7	1	0.45760556	2.42	0.1242
10 VS 6	1	1.35027222	7.13	0.0093
10 VS 1	1	0.47754325	2.52	0.1165
10 VS 4	1	4.32180000	22.83	0.0001
10 VS 3	1	5.73454935	30.29	0.0001
10 VS 2	1	9.73875556	51.44	0.0001
10 VS 5	1	3.26861111	17.26	0.0001
10,9,8,7,6 VS 1,2,3,	1	11.24153526	59.37	0.0001
10,8 VS 1,6,7,9	1	1.56253970	8.25	0.0053
10,8 VS 3,4	1	9.69577795	51.21	0.0001
10,8 VS 2,5	1	11.56437333	61.08	0.0001

General Linear Models Procedure

Dependent Variable: ATTN

Contrast	DF	Contrast SS	F Value	Pr > F
1 VS 9	1	0.47754325	2.52	0.1165
1 VS 8	1	0.00392867	0.02	0.8859
1 VS 7	1	0.00339534	0.02	0.8938
1 VS 6	1	0.15675089	0.83	0.3658
1 VS 4	1	1.57146825	8.30	0.0052
1 VS 3	1	2.48194714	13.11	0.0005
1 VS 2	1	4.96443214	26.22	0.0001
1 VS 5	1	1.10882857	5.86	0.0179
10,9,8,7,1 VS 6,2,3,	1	13.83005524	73.04	0.0001

General Linear Models Procedure

Dependent Variable: ATTN

Contrast	DF	Contrast SS	F Value	Pr > F
2 VS 9	1	9.73875556	51.44	0.0001
2 VS 8	1	5.99733889	31.68	0.0001
2 VS 7	1	5.97427222	31.55	0.0001
2 VS 6	1	3.83645000	20.26	0.0001
2 VS 4	1	1.08535556	5.73	0.0192
2 VS 3	1	0.40047353	2.12	0.1500
2 VS 5	1	1.23480000	6.52	0.0127

General Linear Models Procedure

Dependent Variable: ATTN

Contrast	DF	Contrast SS	F Value	Pr > F
3 VS 9	1	5.73454935	30.29	0.0001
3 VS 8	1	3.03803954	16.05	0.0001
3 VS 7	1	3.02211797	15.96	0.0001
3 VS 6	1	1.60623824	8.48	0.0047
3 VS 4	1	0.14278464	0.75	0.3879
3 VS 5	1	0.23802333	1.26	0.2658

General Linear Models Procedure

Dependent Variable: ATTN

Contrast	DF	Contrast SS	F Value	Pr > F
4 VS 9	1	4.32180000	22.83	0.0001
4 VS 8	1	1.98005000	10.46	0.0018
4 VS 7	1	1.96680556	10.39	0.0019
4 VS 6	1	0.84067222	4.44	0.0384
4 VS 5	1	0.01868611	0.10	0.7543
5 VS 6	1	0.51979375	2.75	0.1017
5 VS 7	1	1.38098819	7.29	0.0085
5 VS 8	1	3.01847778	15.94	0.0002
5 VS 9	1	1.39137153	7.35	0.0083

General Linear Models Procedure

Dependent Variable: ATTN

Contrast	DF	Contrast SS	F Value	Pr > F
6 VS 9	1	0.24035556	1.27	0.2635
6 VS 8	1	1.18067222	6.24	0.0147
6 VS 7	1	0.23575556	1.25	0.2680
7 VS 8	1	0.36125000	1.91	0.1713
7 VS 9	1	0.00002222	0.00	0.9914
8 VS 9	1	0.35560556	1.88	0.1746
4 VS 8	1	4.01388889	21.20	0.0001
4 VS 9	1	1.98005000	10.46	0.0018
5 VS 8	1	5.38945131	28.46	0.0001
3 VS 9	1	3.03803954	16.05	0.0001
2 VS 8	1	9.27368889	48.98	0.0001
2 VS 9	1	5.99733889	31.68	0.0001
1 VS 8	1	0.38500992	2.03	0.1580
1 VS 9	1	0.00392867	0.02	0.8859

Purpose : to find the slope of the linear relation between
center frequency and the depth in 9.18% fat sample

```
1. // JOB
2. // EXEC SAS
3. OPTIONS LS=69;
4. DATA A; INPUT X Y; CARDS;
5. 0.76 2.15
6. 0.95 2.62
7. 1.14 2.62
8. 1.33 2.54
9. 1.52 2.50
10. 1.71 1.56
11. 1.89 2.23
12. 2.08 1.45
13. 2.27 1.45
14. 2.46 1.41
15. 2.65 1.33
16. 0.57 3.16
17. 0.76 3.28
18. 0.95 3.05
19. 1.14 3.16
20. 1.33 2.66
21. 1.52 1.72
22. 1.71 1.72
23. 1.89 1.76
24. 2.08 2.77
25. 0.39 3.16
26. 0.57 3.13
27. 0.76 2.19
28. 0.95 2.62
29. 1.14 2.66
30. 1.32 2.66
31. 1.52 2.62
32. 1.71 1.80
33. 1.89 3.32
34. 2.08 3.36
35. 2.27 2.34
36. 2.46 2.34
37. 0.39 3.09
38. 0.57 2.93
39. 0.76 2.81
40. 0.95 2.93
41. 1.14 1.80
42. 1.33 1.84
43. 1.52 1.84
44. 1.71 1.64
45. 1.89 3.16
46. 2.08 3.16
47. 2.27 3.16
48. 2.46 3.13
49. 0.57 3.32
50. 0.76 3.32
```

51.	0.95	1.95
52.	1.14	1.95
53.	1.33	2.97
54.	1.52	2.93
55.	1.71	2.97
56.	1.89	1.52
57.	2.08	1.52
58.	2.27	1.52
59.	2.46	1.56
60.	2.65	3.01
61.	0.57	2.11
62.	0.76	2.46
63.	0.95	2.42
64.	1.14	2.42
65.	1.33	2.77
66.	1.52	2.42
67.	1.71	2.46
68.	1.89	2.46
69.	2.08	2.50
70.	2.27	2.50
71.	2.46	1.33
72.	2.65	1.37
73.	0.76	3.40
74.	0.95	3.36
75.	1.14	3.36
76.	1.33	3.36
77.	1.52	1.13
78.	1.71	0.90
79.	1.89	3.01
80.	2.08	0.90
81.	2.27	0.94
82.	2.46	1.29
83.	2.65	2.50
84.	0.76	2.85
85.	0.95	2.81
86.	1.14	2.81
87.	1.33	2.81
88.	1.52	3.71
89.	1.71	1.52
90.	1.89	1.48
91.	2.08	1.52
92.	2.27	2.07
93.	2.46	2.07
94.	2.65	2.07
95.	0.57	2.07
96.	0.76	2.07
97.	0.95	2.50
98.	1.14	2.50
99.	1.33	2.58
100.	1.52	3.05
101.	1.71	3.01
102.	1.89	3.01
103.	2.08	2.58
104.	2.27	2.73
105.	2.46	2.03
106.	PROC GLM; CLASS X; MODEL Y=X;	
107.	PROC GLM; MODEL Y=X; OUTPUT P=YHAT R=RESID;	
108.	PROC PRINT;	

General Linear Models Procedure
Class Level Information

Class	Levels	Values
X	14	0.39 0.57 0.76 0.95 1.14 1.32 1.33 1.52 1.71 1.89 2.08 2.27 2.46 2.65

Number of observations in data set = 101

The SAS System 2
14:42 Wednesday, September 25, 1991

General Linear Models Procedure

Dependent Variable: Y

Source	DF	Sum of Squares	F Value	Pr > F
Model	13	10.35148646	1.91	0.0399
Error	87	36.32245611		
Corrected Total	100	46.67394257		
	R-Square	C.V.	Y Mean	
	0.221783	26.90150	2.40188119	

Source	DF	Type I SS	F Value	Pr > F
X	13	10.35148646	1.91	0.0399

Source	DF	Type III SS	F Value	Pr > F
X	13	10.35148646	1.91	0.0399

The SAS System 3
14:42 Wednesday, September 25, 1991

General Linear Models Procedure

Number of observations in data set = 101

The SAS System 4
14:42 Wednesday, September 25, 1991

General Linear Models Procedure

Dependent Variable: Y

Source	DF	Sum of Squares	F Value	Pr > F
Model	1	8.12437080	20.86	0.0001

Error	99	38.54957177		
Corrected Total	100	46.67394257		
	R-Square	C.V.	Y Mean	
	0.174067	25.98009	2.40188119	
Source	DF	Type I SS	F Value	Pr > F
X	1	8.12437080	20.86	0.0001
Source	DF	Type III SS	F Value	Pr > F
X	1	8.12437080	20.86	0.0001
Parameter	Estimate	T for H0: Parameter=0	Pr > T	Std Error of Estimate
INTERCEPT	3.106624313	18.68	0.0001	0.16631203
X	-0.451357360	-4.57	0.0001	0.09881385

The SAS System 5
14:42 Wednesday, September 25, 1991

OBS	X	Y	YHAT	RESID
1	0.76	2.15	2.76359	-0.61359
2	0.95	2.62	2.67783	-0.05783
3	1.14	2.62	2.59208	0.02792
4	1.33	2.54	2.50632	0.03368
5	1.52	2.50	2.42056	0.07944
6	1.71	1.56	2.33480	-0.77480
7	1.89	2.23	2.25356	-0.02356
8	2.08	1.45	2.16780	-0.71780
9	2.27	1.45	2.08204	-0.63204
10	2.46	1.41	1.99629	-0.58629
11	2.65	1.33	1.91053	-0.58053
12	0.57	3.16	2.84935	0.31065
13	0.76	3.28	2.76359	0.51641
14	0.95	3.05	2.67783	0.37217
15	1.14	3.16	2.59208	0.56792
16	1.33	2.66	2.50632	0.15368
17	1.52	1.72	2.42056	-0.70056
18	1.71	1.72	2.33480	-0.61480
19	1.89	1.76	2.25356	-0.49356
20	2.08	2.77	2.16780	0.60220
21	0.39	3.16	2.93059	0.22941
22	0.57	3.13	2.84935	0.28065
23	0.76	2.19	2.76359	-0.57359
24	0.95	2.62	2.67783	-0.05783
25	1.14	2.66	2.59208	0.06792
26	1.32	2.66	2.51083	0.14917
27	1.52	2.62	2.42056	0.19944
28	1.71	1.80	2.33480	-0.53480

29	1.89	3.32	2.25356	1.06644
30	2.08	3.36	2.16780	1.19220
31	2.27	2.34	2.08204	0.25796
32	2.46	2.34	1.99629	0.34371
33	0.39	3.09	2.93059	0.15941
34	0.57	2.93	2.84935	0.08065
35	0.76	2.81	2.76359	0.04641
36	0.95	2.93	2.67783	0.25217
37	1.14	1.80	2.59208	-0.79208
38	1.33	1.84	2.50632	-0.66632
39	1.52	1.84	2.42056	-0.58056
40	1.71	1.64	2.33480	-0.69480
41	1.89	3.16	2.25356	0.90644
42	2.08	3.16	2.16780	0.99220
43	2.27	3.16	2.08204	1.07796
44	2.46	3.13	1.99629	1.13371
45	0.57	3.32	2.84935	0.47065
46	0.76	3.32	2.76359	0.55641
47	0.95	1.95	2.67783	-0.72783
48	1.14	1.95	2.59208	-0.64208
49	1.33	2.97	2.50632	0.46368
50	1.52	2.93	2.42056	0.50944
51	1.71	2.97	2.33480	0.63520
52	1.89	1.52	2.25356	-0.73356
53	2.08	1.52	2.16780	-0.64780
54	2.27	1.52	2.08204	-0.56204
55	2.46	1.56	1.99629	-0.43629

The SAS System

6

14:42 Wednesday, September 25, 1991

OBS	X	Y	YHAT	RESID
56	2.65	3.01	1.91053	1.09947
57	0.57	2.11	2.84935	-0.73935
58	0.76	2.46	2.76359	-0.30359
59	0.95	2.42	2.67783	-0.25783
60	1.14	2.42	2.59208	-0.17208
61	1.33	2.77	2.50632	0.26368
62	1.52	2.42	2.42056	-0.00056
63	1.71	2.46	2.33480	0.12520
64	1.89	2.46	2.25356	0.20644
65	2.08	2.50	2.16780	0.33220
66	2.27	2.50	2.08204	0.41796
67	2.46	1.33	1.99629	-0.66629
68	2.65	1.37	1.91053	-0.54053
69	0.76	3.40	2.76359	0.63641
70	0.95	3.36	2.67783	0.68217
71	1.14	3.36	2.59208	0.76792
72	1.33	3.36	2.50632	0.85368
73	1.52	1.13	2.42056	-1.29056
74	1.71	0.90	2.33480	-1.43480
75	1.89	3.01	2.25356	0.75644
76	2.08	0.90	2.16780	-1.26780
77	2.27	0.94	2.08204	-1.14204
78	2.46	1.29	1.99629	-0.70629
79	2.65	2.50	1.91053	0.58947
80	0.76	2.85	2.76359	0.08641
81	0.95	2.81	2.67783	0.13217
82	1.14	2.81	2.59208	0.21792
83	1.33	2.81	2.50632	0.30368

84	1.52	3.71	2.42056	1.28944
85	1.71	1.52	2.33480	-0.81480
86	1.89	1.48	2.25356	-0.77356
87	2.08	1.52	2.16780	-0.64780
88	2.27	2.07	2.08204	-0.01204
89	2.46	2.07	1.99629	0.07371
90	2.65	2.07	1.91053	0.15947
91	0.57	2.07	2.84935	-0.77935
92	0.76	2.07	2.76359	-0.69359
93	0.95	2.50	2.67783	-0.17783
94	1.14	2.50	2.59208	-0.09208
95	1.33	2.58	2.50632	0.07368
96	1.52	3.05	2.42056	0.62944
97	1.71	3.01	2.33480	0.67520
98	1.89	3.01	2.25356	0.75644
99	2.08	2.58	2.16780	0.41220
100	2.27	2.73	2.08204	0.64796
101	2.46	2.03	1.99629	0.03371

Purpose : to find the slope of a linear relation between
center frequency and the depth in 7.19% fat sample

```
1. // JOB
2. // EXEC SAS
3. OPTIONS LS=65;
4. DATA A; INPUT X Y; CARDS;
5. 0.76 2.89
6. 0.95 1.48
7. 1.14 1.45
8. 1.33 2.85
9. 1.52 2.15
10. 1.71 2.19
11. 1.89 2.19
12. 2.08 2.89
13. 2.27 2.11
14. 0.76 2.81
15. 0.95 2.77
16. 1.14 2.07
17. 1.33 3.20
18. 1.52 3.20
19. 1.71 3.20
20. 1.89 3.13
21. 2.08 3.09
21.1 2.27 3.13
21.2 2.46 3.09
21.3 2.65 1.52
22. 0.76 3.55
23. 0.95 3.75
24. 1.14 2.89
25. 1.33 2.89
26. 1.52 1.05
27. 1.71 1.72
28. 1.89 1.05
29. 2.08 1.72
30. 2.27 2.42
31. 0.95 2.93
32. 1.14 2.34
33. 1.33 1.02
34. 1.52 0.90
35. 1.71 0.90
36. 1.89 0.94
37. 2.08 1.80
38. 2.27 1.84
39. 2.46 3.05
40. 2.65 3.05
41. 2.84 1.64
42. 0.95 2.93
43. 1.14 2.97
44. 1.33 2.62
45. 1.52 2.54
46. 1.71 2.07
47. 1.89 2.50
48. 2.08 2.46
49. 2.27 2.34
50. 2.46 2.34
```

51.	2.65	2.34
52.	2.84	2.34
53.	0.57	1.80
54.	0.76	2.81
55.	0.95	2.85
56.	1.14	2.81
57.	1.33	2.85
58.	1.52	2.81
59.	1.71	1.72
60.	1.89	1.48
61.	2.08	1.48
62.	2.27	1.41
63.	0.57	1.99
64.	0.76	2.73
65.	0.95	2.70
66.	1.14	2.73
67.	1.33	2.70
68.	1.52	2.42
69.	1.71	1.72
70.	1.89	1.56
71.	2.08	1.48
72.	0.39	3.09
73.	0.57	3.13
74.	0.76	3.09
75.	0.95	3.13
76.	1.14	1.68
77.	1.33	1.68
78.	1.52	1.68
79.	1.71	1.72
80.	1.89	3.28
81.	0.76	3.48
82.	0.95	3.32
83.	1.14	2.62
84.	1.33	2.62
85.	1.52	1.41
86.	1.71	2.70
87.	1.89	0.90
88.	2.08	0.90
89.	2.27	0.90
90.	2.46	0.90
91.	2.65	1.76
106.	PROC GLM; CLASS X; MODEL Y=X;	
107.	PROC GLM; MODEL Y=X; OUTPUT P=YHAT R=RESID;	
108.	PROC PRINT;	

General Linear Models Procedure
Class Level Information

Class	Levels	Values
X	14	0.39 0.57 0.76 0.95 1.14 1.33 1.52 1.71 1.89 2.08 2.27 2.46 2.65 2.84

Number of observations in data set = 90

The SAS System 2
15:36 Wednesday, September 25, 1991

General Linear Models Procedure

Dependent Variable: Y

Source	DF	Sum of Squares	F Value	Pr > F
Model	13	12.65075357	1.93	0.0400
Error	76	38.41465198		
Corrected Total	89	51.06540556		

R-Square	C.V.	Y Mean
0.247736	31.00842	2.29277778

Source	DF	Type I SS	F Value	Pr > F
X	13	12.65075357	1.93	0.0400

Source	DF	Type III SS	F Value	Pr > F
X	13	12.65075357	1.93	0.0400

The SAS System 3
15:36 Wednesday, September 25, 1991

General Linear Models Procedure

Number of observations in data set = 90

The SAS System 4
15:36 Wednesday, September 25, 1991

General Linear Models Procedure

Dependent Variable: Y

Source	DF	Sum of Squares	F Value	Pr > F
Model	1	6.51103613	12.86	0.0006

Error	88	44.55436943		
Corrected Total	89	51.06540556		
	R-Square	C.V.	Y Mean	
	0.127504	31.03429	2.29277778	

Source	DF	Type I SS	F Value	Pr > F
X	1	6.51103613	12.86	0.0006

Source	DF	Type III SS	F Value	Pr > F
X	1	6.51103613	12.86	0.0006

Parameter	Estimate	T for H0: Parameter=0	Pr > T	Std Error of Estimate
INTERCEPT	3.005926529	14.14	0.0001	0.21253926
X	-0.449054696	-3.59	0.0006	0.12522124

The SAS System 5
15:36 Wednesday, September 25, 1991

OBS	X	Y	YHAT	RESID
1	0.76	2.89	2.66464	0.22536
2	0.95	1.48	2.57932	-1.09932
3	1.14	1.45	2.49400	-1.04400
4	1.33	2.85	2.40868	0.44132
5	1.52	2.15	2.32336	-0.17336
6	1.71	2.19	2.23804	-0.04804
7	1.89	2.19	2.15721	0.03279
8	2.08	2.89	2.07189	0.81811
9	2.27	2.11	1.98657	0.12343
10	0.76	2.81	2.66464	0.14536
11	0.95	2.77	2.57932	0.19068
12	1.14	2.07	2.49400	-0.42400
13	1.33	3.20	2.40868	0.79132
14	1.52	3.20	2.32336	0.87664
15	1.71	3.20	2.23804	0.96196
16	1.89	3.13	2.15721	0.97279
17	2.08	3.09	2.07189	1.01811
18	2.27	3.13	1.98657	1.14343
19	2.46	3.09	1.90125	1.18875
20	2.65	1.52	1.81593	-0.29593
21	0.76	3.55	2.66464	0.88536
22	0.95	3.75	2.57932	1.17068
23	1.14	2.89	2.49400	0.39600
24	1.33	2.89	2.40868	0.48132
25	1.52	1.05	2.32336	-1.27336
26	1.71	1.72	2.23804	-0.51804
27	1.89	1.05	2.15721	-1.10721
28	2.08	1.72	2.07189	-0.35189

29	2.27	2.42	1.98657	0.43343
30	0.95	2.93	2.57932	0.35068
31	1.14	2.34	2.49400	-0.15400
32	1.33	1.02	2.40868	-1.38868
33	1.52	0.90	2.32336	-1.42336
34	1.71	0.90	2.23804	-1.33804
35	1.89	0.94	2.15721	-1.21721
36	2.08	1.80	2.07189	-0.27189
37	2.27	1.84	1.98657	-0.14657
38	2.46	3.05	1.90125	1.14875
39	2.65	3.05	1.81593	1.23407
40	2.84	1.64	1.73061	-0.09061
41	0.95	2.93	2.57932	0.35068
42	1.14	2.97	2.49400	0.47600
43	1.33	2.62	2.40868	0.21132
44	1.52	2.54	2.32336	0.21664
45	1.71	2.07	2.23804	-0.16804
46	1.89	2.50	2.15721	0.34279
47	2.08	2.46	2.07189	0.38811
48	2.27	2.34	1.98657	0.35343
49	2.46	2.34	1.90125	0.43875
50	2.65	2.34	1.81593	0.52407
51	2.84	2.34	1.73061	0.60939
52	0.57	1.80	2.74997	-0.94997
53	0.76	2.81	2.66464	0.14536
54	0.95	2.85	2.57932	0.27068
55	1.14	2.81	2.49400	0.31600

The SAS System

6

15:36 Wednesday, September 25, 1991

OBS	X	Y	YHAT	RESID
56	1.33	2.85	2.40868	0.44132
57	1.52	2.81	2.32336	0.48664
58	1.71	1.72	2.23804	-0.51804
59	1.89	1.48	2.15721	-0.67721
60	2.08	1.48	2.07189	-0.59189
61	2.27	1.41	1.98657	-0.57657
62	0.57	1.99	2.74997	-0.75997
63	0.76	2.73	2.66464	0.06536
64	0.95	2.70	2.57932	0.12068
65	1.14	2.73	2.49400	0.23600
66	1.33	2.70	2.40868	0.29132
67	1.52	2.42	2.32336	0.09664
68	1.71	1.72	2.23804	-0.51804
69	1.89	1.56	2.15721	-0.59721
70	2.08	1.48	2.07189	-0.59189
71	0.39	3.09	2.83080	0.25920
72	0.57	3.13	2.74997	0.38003
73	0.76	3.09	2.66464	0.42536
74	0.95	3.13	2.57932	0.55068
75	1.14	1.68	2.49400	-0.81400
76	1.33	1.68	2.40868	-0.72868
77	1.52	1.68	2.32336	-0.64336
78	1.71	1.72	2.23804	-0.51804
79	1.89	3.28	2.15721	1.12279
80	0.76	3.48	2.66464	0.81536
81	0.95	3.32	2.57932	0.74068
82	1.14	2.62	2.49400	0.12600
83	1.33	2.62	2.40868	0.21132

84	1.52	1.41	2.32336	-0.91336
85	1.71	2.70	2.23804	0.46196
86	1.89	0.90	2.15721	-1.25721
87	2.08	0.90	2.07189	-1.17189
88	2.27	0.90	1.98657	-1.08657
89	2.46	0.90	1.90125	-1.00125
90	2.65	1.76	1.81593	-0.05593

Purpose : to find the slope of a linear relation between
center frequency and depth in 5.12% fat sample

```
1. // JOB
2. // EXEC SAS
3. OPTIONS LS=65;
4. DATA A; INPUT X Y; CARDS;
5. 0.39 3.52
6. 0.57 3.52
7. 0.76 2.46
8. 0.95 2.42
9. 1.14 2.42
10. 1.33 2.46
11. 1.52 2.42
12. 1.71 2.27
13. 1.89 1.68
14. 2.08 1.64
15. 2.27 1.64
16. 0.57 3.44
17. 0.76 2.81
18. 0.95 2.70
19. 1.14 2.42
20. 1.33 1.09
21. 1.52 2.11
21.1 1.71 1.72
21.2 1.89 2.15
21.3 2.08 0.82
22. 2.27 1.76
23. 2.46 0.82
24. 0.76 3.24
25. 0.95 3.52
26. 1.14 3.55
27. 1.33 3.20
28. 1.52 2.30
29. 1.71 2.30
30. 1.89 0.94
31. 2.08 1.68
32. 2.27 2.11
33. 2.46 2.11
34. 2.65 2.11
35. 2.84 2.03
36. 0.57 3.01
37. 0.76 2.97
38. 0.95 3.01
39. 1.14 1.48
40. 1.33 3.20
41. 1.52 3.20
42. 1.71 3.20
43. 1.89 1.60
44. 2.08 1.68
45. 2.27 1.68
46. 2.46 1.80
47. 2.65 1.84
48. 0.57 2.66
49. 0.76 2.70
50. 0.95 2.66
```

51.	1.14	2.70
52.	1.33	1.45
53.	1.52	1.48
54.	1.71	1.52
55.	1.89	2.81
56.	2.08	2.85
57.	2.27	2.46
58.	2.46	2.46
59.	0.57	2.46
60.	0.76	2.46
61.	0.95	2.07
62.	1.14	2.03
63.	1.33	2.03
64.	1.52	2.11
65.	1.71	2.97
66.	1.89	1.02
67.	2.08	2.23
68.	2.27	1.09
69.	0.76	3.01
70.	0.95	3.01
71.	1.14	3.01
72.	1.33	3.01
73.	1.52	1.02
74.	1.71	0.90
75.	1.89	0.90
76.	2.08	1.13
77.	2.27	1.05
78.	0.95	2.23
79.	1.14	2.23
80.	1.33	1.13
81.	1.52	1.13
82.	1.71	1.09
83.	1.89	0.74
84.	2.08	1.52
85.	2.27	1.52
86.	2.46	0.82
87.	0.95	2.81
88.	1.14	1.68
89.	1.33	1.68
90.	1.52	1.68
91.	1.71	0.74
92.	1.89	0.70
93.	2.08	1.91
94.	2.27	0.66
95.	2.46	0.86
106.	PROC GLM; CLASS X; MODEL Y=X;	
107.	PROC GLM; MODEL Y=X; OUTPUT P=YHAT R=RESID;	
108.	PROC PRINT;	

General Linear Models Procedure
Class Level Information

Class	Levels	Values
X	14	0.39 0.57 0.76 0.95 1.14 1.33 1.52 1.71 1.89 2.08 2.27 2.46 2.65 2.84

Number of observations in data set = 94

The SAS System 2
16:07 Wednesday, September 25, 1991

General Linear Models Procedure

Dependent Variable: Y

Source	DF	Sum of Squares	F Value	Pr > F
Model	13	25.44263530	4.54	0.0001
Error	80	34.47255619		
Corrected Total	93	59.91519149		
	R-Square	C.V.	Y Mean	
	0.424644	31.73467	2.06851064	

Source	DF	Type I SS	F Value	Pr > F
X	13	25.44263530	4.54	0.0001
Source	DF	Type III SS	F Value	Pr > F
X	13	25.44263530	4.54	0.0001

The SAS System 3
16:07 Wednesday, September 25, 1991

General Linear Models Procedure

Number of observations in data set = 94

The SAS System 4
16:07 Wednesday, September 25, 1991

General Linear Models Procedure

Dependent Variable: Y

Source	DF	Sum of Squares	F Value	Pr > F
Model	1	20.47489389	47.76	0.0001

Error	92	39.44029760		
Corrected Total	93	59.91519149		
	R-Square	C.V.	Y Mean	
	0.341731	31.65326	2.06851064	

Source	DF	Type I SS	F Value	Pr > F
X	1	20.47489389	47.76	0.0001
Source	DF	Type III SS	F Value	Pr > F
X	1	20.47489389	47.76	0.0001

Parameter	Estimate	T for H0: Parameter=0	Pr > T	Std Error of Estimate
INTERCEPT	3.300590143	17.31	0.0001	0.19064259
X	-0.785349383	-6.91	0.0001	0.11363922

The SAS System 5
16:07 Wednesday, September 25, 1991

OBS	X	Y	YHAT	RESID
1	0.39	3.52	2.99430	0.52570
2	0.57	3.52	2.85294	0.66706
3	0.76	2.46	2.70372	-0.24372
4	0.95	2.42	2.55451	-0.13451
5	1.14	2.42	2.40529	0.01471
6	1.33	2.46	2.25608	0.20392
7	1.52	2.42	2.10686	0.31314
8	1.71	2.27	1.95764	0.31236
9	1.89	1.68	1.81628	-0.13628
10	2.08	1.64	1.66706	-0.02706
11	2.27	1.64	1.51785	0.12215
12	0.57	3.44	2.85294	0.58706
13	0.76	2.81	2.70372	0.10628
14	0.95	2.70	2.55451	0.14549
15	1.14	2.42	2.40529	0.01471
16	1.33	1.09	2.25608	-1.16608
17	1.52	2.11	2.10686	0.00314
18	1.71	1.72	1.95764	-0.23764
19	1.89	2.15	1.81628	0.33372
20	2.08	0.82	1.66706	-0.84706
21	2.27	1.76	1.51785	0.24215
22	2.46	0.82	1.36863	-0.54863
23	0.76	3.24	2.70372	0.53628
24	0.95	3.52	2.55451	0.96549
25	1.14	3.55	2.40529	1.14471
26	1.33	3.20	2.25608	0.94392
27	1.52	2.30	2.10686	0.19314
28	1.71	2.30	1.95764	0.34236

29	1.89	0.94	1.81628	-0.87628
30	2.08	1.68	1.66706	0.01294
31	2.27	2.11	1.51785	0.59215
32	2.46	2.11	1.36863	0.74137
33	2.65	2.11	1.21941	0.89059
34	2.84	2.03	1.07020	0.95980
35	0.57	3.01	2.85294	0.15706
36	0.76	2.97	2.70372	0.26628
37	0.95	3.01	2.55451	0.45549
38	1.14	1.48	2.40529	-0.92529
39	1.33	3.20	2.25608	0.94392
40	1.52	3.20	2.10686	1.09314
41	1.71	3.20	1.95764	1.24236
42	1.89	1.60	1.81628	-0.21628
43	2.08	1.68	1.66706	0.01294
44	2.27	1.68	1.51785	0.16215
45	2.46	1.80	1.36863	0.43137
46	2.65	1.84	1.21941	0.62059
47	0.57	2.66	2.85294	-0.19294
48	0.76	2.70	2.70372	-0.00372
49	0.95	2.66	2.55451	0.10549
50	1.14	2.70	2.40529	0.29471
51	1.33	1.45	2.25608	-0.80608
52	1.52	1.48	2.10686	-0.62686
53	1.71	1.52	1.95764	-0.43764
54	1.89	2.81	1.81628	0.99372
55	2.08	2.85	1.66706	1.18294

The SAS System

6

16:07 Wednesday, September 25, 1991

OBS	X	Y	YHAT	RESID
56	2.27	2.46	1.51785	0.94215
57	2.46	2.46	1.36863	1.09137
58	0.57	2.46	2.85294	-0.39294
59	0.76	2.46	2.70372	-0.24372
60	0.95	2.07	2.55451	-0.48451
61	1.14	2.03	2.40529	-0.37529
62	1.33	2.03	2.25608	-0.22608
63	1.52	2.11	2.10686	0.00314
64	1.71	2.97	1.95764	1.01236
65	1.89	1.02	1.81628	-0.79628
66	2.08	2.23	1.66706	0.56294
67	2.27	1.09	1.51785	-0.42785
68	0.76	3.01	2.70372	0.30628
69	0.95	3.01	2.55451	0.45549
70	1.14	3.01	2.40529	0.60471
71	1.33	3.01	2.25608	0.75392
72	1.52	1.02	2.10686	-1.08686
73	1.71	0.90	1.95764	-1.05764
74	1.89	0.90	1.81628	-0.91628
75	2.08	1.13	1.66706	-0.53706
76	2.27	1.05	1.51785	-0.46785
77	0.95	2.23	2.55451	-0.32451
78	1.14	2.23	2.40529	-0.17529
79	1.33	1.13	2.25608	-1.12608
80	1.52	1.13	2.10686	-0.97686
81	1.71	1.09	1.95764	-0.86764
82	1.89	0.74	1.81628	-1.07628
83	2.08	1.52	1.66706	-0.14706

84	2.27	1.52	1.51785	0.00215
85	2.46	0.82	1.36863	-0.54863
86	0.95	2.81	2.55451	0.25549
87	1.14	1.68	2.40529	-0.72529
88	1.33	1.68	2.25608	-0.57608
89	1.52	1.68	2.10686	-0.42686
90	1.71	0.74	1.95764	-1.21764
91	1.89	0.70	1.81628	-1.11628
92	2.08	1.91	1.66706	0.24294
93	2.27	0.66	1.51785	-0.85785
94	2.46	0.86	1.36863	-0.50863

Purpose : to find the slope of a linear relation between
attenuation slope and fat

```
1. // JOB
2. // EXEC SAS
3. OPTIONS LS=69;
4. DATA A; INPUT X Y; CARDS;
5. 10.88 2.35
6. 10.88 2.03
7. 10.88 2.36
8. 10.88 1.90
9. 10.88 2.27
10. 10.88 1.51
11. 10.88 2.85
12. 10.88 2.41
13. 10.88 3.03
14. 9.45 1.66
15. 9.45 2.63
16. 9.45 1.95
17. 9.45 1.87
18. 9.45 2.15
19. 9.45 2.21
20. 9.45 1.29
21. 9.45 1.71
22. 9.45 2.39
23. 9.18 2.47
24. 9.18 1.89
25. 9.18 3.30
26. 9.18 1.62
27. 9.18 2.86
28. 9.18 2.40
29. 9.18 2.17
30. 9.18 2.17
31. 9.18 1.51
32. 8.85 1.57
33. 8.85 1.45
34. 8.85 1.70
35. 8.85 2.46
36. 8.85 1.88
37. 8.85 2.94
38. 8.85 1.68
39. 8.85 2.18
40. 8.85 1.98
41. 7.19 1.66
42. 7.19 1.88
43. 7.19 1.86
44. 7.19 2.03
45. 7.19 1.71
46. 7.19 1.16
47. 7.19 1.86
48. 7.19 1.91
49. 7.19 1.71
50. 5.20 1.62
```

51.	5.20	1.62
52.	5.20	2.67
53.	5.20	1.63
54.	5.20	1.42
55.	5.20	2.75
56.	5.20	1.96
57.	3.56	1.55
58.	3.56	1.11
59.	3.56	1.74
60.	3.56	1.16
61.	3.56	1.16
62.	3.56	1.18
63.	3.56	1.83
64.	2.74	1.01
65.	2.74	1.26
66.	2.74	1.64
67.	2.74	1.79
68.	2.74	1.82
69.	2.74	0.57
70.	2.74	0.85
71.	2.74	1.20
72.	2.74	1.75
73.	2.28	0.99
74.	2.28	1.12
75.	2.28	0.86
76.	2.28	1.17
77.	2.28	0.82
78.	2.28	0.80
79.	2.28	1.37
80.	2.28	1.97
81.	1.52	0.59
82.	1.52	0.36
83.	1.52	1.30
84.	1.52	0.51
85.	1.52	0.99
86.	1.52	0.33
87.	1.52	1.11
88.	1.52	1.18
89.	1.52	1.10
106.	PROC GLM; CLASS X; MODEL Y=X;	
107.	PROC GLM; MODEL Y=X; OUTPUT P=YHAT R=RESID;	
108.	PROC PRINT;	

General Linear Models Procedure
Class Level Information

Class	Levels	Values
X	10	5.2 1.52 2.28 2.74 3.56 7.19 8.85 9.18 9.45 10.88

Number of observations in data set = 85

The SAS System 2
15:04 Sunday, October 13, 1991

General Linear Models Procedure

Dependent Variable: Y

Source	DF	Sum of Squares	F Value	Pr > F
Model	9	19.35688701	11.36	0.0001
Error	75	14.20047063		
Corrected Total	84	33.55735765		

R-Square	C.V.	Y Mean
0.576830	25.60662	1.69929412

Source	DF	Type I SS	F Value	Pr > F
X	9	19.35688701	11.36	0.0001

Source	DF	Type III SS	F Value	Pr > F
X	9	19.35688701	11.36	0.0001

The SAS System 3
15:04 Sunday, October 13, 1991

General Linear Models Procedure

Number of observations in data set = 85

The SAS System 4
15:04 Sunday, October 13, 1991

General Linear Models Procedure

Dependent Variable: Y

Source	DF	Sum of Squares	F Value	Pr > F
Model	1	17.12826818	86.53	0.0001

Error	83	16.42908946		
Corrected Total	84	33.55735765		
	R-Square	C.V.		Y Mean
	0.510418	26.18178		1.69929412

Source	DF	Type I SS	F Value	Pr > F
X	1	17.12826818	86.53	0.0001

Source	DF	Type III SS	F Value	Pr > F
X	1	17.12826818	86.53	0.0001

Parameter	Estimate	T for H0: Parameter=0	Pr > T	Std Error of Estimate
INTERCEPT	0.8554875322	8.33	0.0001	0.10274712
X	0.1358786772	9.30	0.0001	0.01460704

The SAS System 5
15:04 Sunday, October 13, 1991

OBS	X	Y	YHAT	RESID
1	10.88	2.35	2.33385	0.01615
2	10.88	2.03	2.33385	-0.30385
3	10.88	2.36	2.33385	0.02615
4	10.88	1.90	2.33385	-0.43385
5	10.88	2.27	2.33385	-0.06385
6	10.88	1.51	2.33385	-0.82385
7	10.88	2.85	2.33385	0.51615
8	10.88	2.41	2.33385	0.07615
9	10.88	3.03	2.33385	0.69615
10	9.45	1.66	2.13954	-0.47954
11	9.45	2.63	2.13954	0.49046
12	9.45	1.95	2.13954	-0.18954
13	9.45	1.87	2.13954	-0.26954
14	9.45	2.15	2.13954	0.01046
15	9.45	2.21	2.13954	0.07046
16	9.45	1.29	2.13954	-0.84954
17	9.45	1.71	2.13954	-0.42954
18	9.45	2.39	2.13954	0.25046
19	9.18	2.47	2.10285	0.36715
20	9.18	1.89	2.10285	-0.21285
21	9.18	3.30	2.10285	1.19715
22	9.18	1.62	2.10285	-0.48285
23	9.18	2.86	2.10285	0.75715
24	9.18	2.40	2.10285	0.29715
25	9.18	2.17	2.10285	0.06715
26	9.18	2.17	2.10285	0.06715
27	9.18	1.51	2.10285	-0.59285
28	8.85	1.57	2.05801	-0.48801

29	8.85	1.45	2.05801	-0.60801
30	8.85	1.70	2.05801	-0.35801
31	8.85	2.46	2.05801	0.40199
32	8.85	1.88	2.05801	-0.17801
33	8.85	2.94	2.05801	0.88199
34	8.85	1.68	2.05801	-0.37801
35	8.85	2.18	2.05801	0.12199
36	8.85	1.98	2.05801	-0.07801
37	7.19	1.66	1.83246	-0.17246
38	7.19	1.88	1.83246	0.04754
39	7.19	1.86	1.83246	0.02754
40	7.19	2.03	1.83246	0.19754
41	7.19	1.71	1.83246	-0.12246
42	7.19	1.16	1.83246	-0.67246
43	7.19	1.86	1.83246	0.02754
44	7.19	1.91	1.83246	0.07754
45	7.19	1.71	1.83246	-0.12246
46	5.20	1.62	1.56206	0.05794
47	5.20	1.62	1.56206	0.05794
48	5.20	2.67	1.56206	1.10794
49	5.20	1.63	1.56206	0.06794
50	5.20	1.42	1.56206	-0.14206
51	5.20	2.75	1.56206	1.18794
52	5.20	1.96	1.56206	0.39794
53	3.56	1.55	1.33922	0.21078
54	3.56	1.11	1.33922	-0.22922
55	3.56	1.74	1.33922	0.40078

The SAS System

6

15:04 Sunday, October 13, 1991

OBS	X	Y	YHAT	RESID
56	3.56	1.16	1.33922	-0.17922
57	3.56	1.16	1.33922	-0.17922
58	3.56	1.18	1.33922	-0.15922
59	3.56	1.83	1.33922	0.49078
60	2.74	1.01	1.22780	-0.21780
61	2.74	1.26	1.22780	0.03220
62	2.74	1.64	1.22780	0.41220
63	2.74	1.79	1.22780	0.56220
64	2.74	1.82	1.22780	0.59220
65	2.74	0.57	1.22780	-0.65780
66	2.74	0.85	1.22780	-0.37780
67	2.74	1.20	1.22780	-0.02780
68	2.74	1.75	1.22780	0.52220
69	2.28	0.99	1.16529	-0.17529
70	2.28	1.12	1.16529	-0.04529
71	2.28	0.86	1.16529	-0.30529
72	2.28	1.17	1.16529	0.00471
73	2.28	0.82	1.16529	-0.34529
74	2.28	0.80	1.16529	-0.36529
75	2.28	1.37	1.16529	0.20471
76	2.28	1.97	1.16529	0.80471
77	1.52	0.59	1.06202	-0.47202
78	1.52	0.36	1.06202	-0.70202
79	1.52	1.30	1.06202	0.23798
80	1.52	0.51	1.06202	-0.55202
81	1.52	0.99	1.06202	-0.07202
82	1.52	0.33	1.06202	-0.73202
83	1.52	1.11	1.06202	0.04798
84	1.52	1.18	1.06202	0.11798
85	1.52	1.10	1.06202	0.03798